

Autoimmunity is a Significant Feature of Idiopathic Pulmonary Arterial Hypertension

Rowena J. Jones (1)*; Eckart M.D.D. De Bie (1)*; Emily Groves (1)*; Kasia I. Zalewska (1, 2); Emilia M. Swietlik (1, 2); Carmen M. Treacy (1); Jennifer M. Martin (1); Gary Polwarth (2); Wei Li (1); Jingxu Guo (1); Helen E. Baxendale (2); Stephen Coleman (3); Natalia Savinykh (4); J. Gerry Coghlan (5); Paul A. Corris (6); Luke S. Howard (7); Martin K. Johnson (8); Colin Church (8); David G. Kiely (9); Allan Lawrie (10); James L. Lordan (6); Robert V. Mackenzie Ross (11); Joanna Pepke Zaba (2); Martin R. Wilkins (12); S. John Wort (13); Edoardo Fiorillo (14); Valeria Orrù (14); Francesco Cucca (15); Christopher J. Rhodes (12); Stefan Gräf (1); Nicholas W. Morrell (1); Eoin F. McKinney (16); Chris Wallace (1, 3 & 16)*; Mark Toshner (1&2)*

The UK National PAH Cohort Study Consortium

*Authors contributed equally to the manuscript

Corresponding author: Mark Toshner, MD.

Department of Medicine,

University of Cambridge,

Addenbrookes Hospital,

Cambridge, UK, CB2 0QQ

mrt34@medschl.cam.ac.uk

- 1) Heart and Lung Research Institute, Department of Medicine, University of Cambridge
School of Clinical Medicine, Addenbrookes Hospital, Cambridge, UK
- 2) Royal Papworth Hospital, Cambridge Biomedical Campus, Cambridge, UK
- 3) MRC Biostatistics Unit, Cambridge Biomedical Campus, Cambridge, UK

- 4) Cambridge BRC Phenotyping Hub, Department of Medicine, University of Cambridge., UK
- 5) Royal Free London NHS Foundation Trust, London, UK
- 6) Freeman Hospital, Newcastle-upon-Tyne, UK
- 7) Hammersmith Hospital, London, UK
- 8) Scottish Pulmonary Vascular Unit, Golden Jubilee National Hospital, Glasgow, UK
- 9) Sheffield Pulmonary Vascular Disease Unit, Royal Hallamshire Hospital, Sheffield, UK
- 10) Department of Infection, Immunity and Cardiovascular Disease, University of Sheffield, UK
- 11) Royal United Hospitals Bath NHS Foundation Trust, Bath, UK
- 12) National Heart and Lung Institute, Medicine, Imperial College London, London, UK
- 13) Royal Brompton Hospital, London, UK
- 14) Istituto di Ricerca Genetica e Biomedica, Consiglio Nazionale delle Ricerche (CNR), Cagliari, Italy.
- 15) University of Sassari, Sassari, Italy.
- 16) Cambridge Institute of Therapeutic Immunology and Infectious Disease, Jeffrey Cheah Biomedical Centre, Cambridge Biomedical Campus, Cambridge, UK

This article has an online data supplement, which is accessible from this issue's table of content online at www.atsjournals.org.

Author Contributions

R.J.J., E.M.D.D.D., E.G., K.I.Z., S.G., E.F.M., J.G., W.L., H.B., N.S., C.W., and M.T. undertook study design, data analysis and interpretation. R.J.J., E.M.D.D.D., C.W. and M.T. wrote the original article. E.M.S., S.C. and C.J.R. assisted with data curation. C.M.T. J.M.M,

G.P, J.G.C., C.C., P.A.C., L.S.H., M.K.J., D.G.K., A.L., J.L.L., R.V.M-R., J.P-Z., M.R.W., S.J.W., N.W.M., and M.T. represent the UK National PAH Study Consortium and assisted with samples and study conceptualisation. E.F., V.O. and F.C. provided control samples.

All authors provided constructive criticism of the study manuscript.

Funding

All funders were restricted to financial support. The NIHR BRC, MRC (MC_UU_00002/4) and Wellcome Trust [WT107881] supported salary costs. The Dinosaur Trust provided funding for a PhD studentship. The UK National Cohort of Idiopathic and Heritable PAH is supported by the NIHR, the British Heart Foundation (BHF, SP/12/12/29836), the BHF Imperial Centre of Cardiovascular Research Excellence (RE/18/4/34215), the BHF Cambridge Centre of Cardiovascular Research Excellence, the UK Medical Research Council (MR/K020919/1), the Dinosaur Trust, NIHR Great Ormond Street Hospital Biomedical Research Centre and Great Ormond Street Hospital Charity. A.L. is supported by a BHF Senior Basic Science Research fellowship (FS/18/52/33808).

Running title: Autoimmunity in idiopathic PAH.

Descriptor number: 9.35

Word Count: 3315

Impact of research: To our knowledge this is the largest ever study into the significance of autoimmunity in idiopathic and heritable pulmonary arterial hypertension (PAH), and shows that using multiple methodological approaches, idiopathic PAH displays an autoimmune signature. The association of autoimmunity with IPAH has important therapeutic implications. Further work is required to understand the longitudinal variability within the disease and how

this might translate into stratification of patient endotypes for the purpose of personalised medicine in future clinical trials.

This article is open access and distributed under the terms of the Creative Commons Attribution 4.0 International License (<https://creativecommons.org/licenses/by/4.0/>).

At A Glance

What is the current scientific knowledge on this subject?

Whilst PAH is known to have a multitude of causes, the cause of IPAH and its association with autoimmunity has been a topic of debate.

What does this study add to the field?

To our knowledge this is the largest ever study into the significance of autoimmunity in idiopathic and heritable pulmonary arterial hypertension (PAH), and shows that using multiple methodological approaches, idiopathic PAH displays an autoimmune signature. The association of autoimmunity with IPAH has important therapeutic implications.

Abstract

Rationale: Autoimmunity is thought to play a role in idiopathic pulmonary arterial hypertension (IPAH). It is not clear if this is causative or a bystander of disease and if it carries any prognostic or treatment significance.

Objective: To study autoimmunity in IPAH using a large cross-sectional cohort.

Methods: Assessment of the circulating immune cell phenotype was undertaken using flow cytometry and the profile of serum immunoglobulins was generated using a standardised multiplex array of 19 clinically validated autoantibodies in 473 cases and 946 controls. Additional GST-fusion array and ELISA data were used to identify a serum autoantibody to BMPR2. Clustering analyses and clinical correlations were employed to determine associations between immunogenicity and clinical outcomes.

Measurements and Main Results: Flow cytometric immune profiling demonstrates IPAH is associated with an altered humoral immune response in addition to raised IgG3. Multiplexed autoantibodies were significantly raised in IPAH, and clustering demonstrated three distinct clusters: ‘high autoantibody’, ‘low autoantibody’, and a small ‘intermediate’ cluster exhibiting high levels of RNP-complex. The high autoantibody cluster had worse haemodynamics but improved survival. A small subset of patients demonstrated immunoglobulin reactivity to BMPR2.

Conclusions: This study establishes aberrant immune regulation and presence of autoantibodies as a key feature in the profile of a significant proportion of IPAH patients and is associated with clinical outcomes.

Word Count: 215 words.

Key Words: Autoimmune, pulmonary arterial hypertension, IPAH, BMPR2, autoantibodies, immunophenotyping.

Introduction

Pulmonary arterial hypertension (PAH) is characterised by severe remodelling of the pulmonary arteries causing increased pulmonary vascular resistance and resulting in reduced cardiac output, right heart failure and despite the availability of numerous licensed therapies, a reduced life expectancy (1). PAH is a mixed classification of pathologies, with a well-recognised female predominance, and has known associations with female prevalent autoimmune diseases, including systemic sclerosis-PAH (SSc-PAH), systemic lupus erythematosus (SLE) and Sjögren's syndrome (2). The most common specialist centre diagnosis remains idiopathic PAH (IPAH) where the cause is still undetermined. Patients with IPAH show overlap features of autoimmune disease including inflammation and immune cell infiltration within the lung, and putative circulating auto-antibodies (1, 3–6). The concept that IPAH represents an undiagnosed autoimmune disease has circulated for decades (3, 7). The availability of whole genome sequencing has clarified that only a modest proportion of patients with IPAH are likely to be reclassified as having a rare disease-causing mutation, but adding weight to the autoimmune hypothesis, the major signal from common genetic variant analysis was located in an HLA associated locus (8) and most recently, unsupervised clustering of whole blood transcriptomics identified differences between immunoglobulin transcription as a determinant of good and poor surviving clusters of patients with IPAH (9). Irrespective of the causal versus associative nature of autoimmunity or inflammation, it remains an attractive target for drug repurposing. To date, no trial has successfully identified responders to immunomodulator therapies. A better understanding of the nature and proportion of patients with dysregulated immunity in IPAH is necessary to guide pathophysiology studies and future therapeutic trials.

Herein we describe the circulating immune phenotype and autoantibody profiling in PAH utilising patient samples collected as part of the UK National cohort study of Idiopathic and Heritable PAH. We demonstrate that autoimmunity is associated with IPAH using a number of differing techniques in the largest study to date where autoimmunity clustering was associated with clinical phenotypes and outcomes. We also identify an uncommon putative autoantibody to the TGF β superfamily receptor, BMPR2, a key functional protein in PAH biology (10).

Methods

Subjects and ethical consent

All samples and data were obtained with written informed consent. Patients diagnosed with heritable and idiopathic PAH, pulmonary veno-occlusive disease (PVOD) or pulmonary capillary hemangiomatosis (PCH) according to WHO classification and aged >18 years were recruited to the wider cohort study as previously described (8, 11).

For the immunophenotyping study, subjects were additionally recruited from the Pulmonary Vascular Diseases Unit at the Royal Papworth Hospital under the Papworth Hospital Tissue Bank (Donation for the collection and storage of human biological material for research; Cambridgeshire East Research Ethics Committee reference 08/H0304/56, tissue bank project number T01990). Patient and control subjects for the autoantibody studies were recruited from the UK National cohort study of Idiopathic and Hereditary PAH (13/EE/0203; NCT01907295) and further controls were recruited from the ‘Genetics and epidemiology of aging-associated conditions’, (ProgeNIA PROT 2171/CE) and ‘An integrated approach to dissect the determinants, risk factors and pathways of ageing in the immune system’ (15/EE/0327, IRAS # 188383). Serum samples were collected by the UK National cohort study of Idiopathic and Hereditary PAH between February 2014 and August 2018. Patients were censored in February

2021 using National Health Service records. Additional serum controls from healthy volunteers were used from the StratosPHere study (Optimal biomarkers to ascertain target engagement in therapies targeting the BMPR2 pathway in Pulmonary Arterial Hypertension (PAH), 21/EE/0043). Serum samples were collected in serum SST blood tubes, clotted for 30 minutes, and then centrifuged at 1500 x g for 15 minutes, aliquots were stored at -80°C until required.

Peripheral blood mononuclear fraction collection and immunophenotyping

Peripheral blood mononuclear fractions (PBMCs) were generated by density gradient centrifugation using Ficoll-Paque PLUS (GE Healthcare) from peripheral venous blood in 26 patients with IPAH and 29 healthy controls. Age and sex matching with healthy controls was undertaken on a 1:1 basis with 3 patient samples being excluded because of technically low-quality specific antibody staining. Immunophenotyping was performed using flow cytometry on fresh samples. Antibody staining panels and gating strategy were designed to detect populations of myeloid, B-cells and T cells based upon gating strategies proposed by the Human Immune Consortium (12) and are described in the supplement (See supplementary Tables E1 and E2 and supplementary Figure E1). PBMCs were blocked with Fc block (Miltenyi Bio) and stained with LIVEDEAD (Thermo Scientific) prior to antibody staining for 20 minutes at 4°C. Stained samples were fixed in FACS fixative (1% Formaldehyde, PBS). Samples were analysed using a BD LSRFortessa analyser (BD Bioscience) and analysed using FlowJo software (v 10.0.7). Additional details on the statistical analysis and quantification of immunoglobulin levels and interleukin-21 are provided in an online supplement.

Autoimmune autoantibody quantitation in IPAH and HPAH patients.

A screen of sera from 473 PAH patients and 946 age and sex propensity matched healthy donor controls (1:2 ratio using the MatchIt package v3.0.2) were analysed for the presence of 19 well

characterised, autoimmune disease-associated autoantibodies using an IgG multiplex MagPlex particle-based flow cytometry assay (ProtoPlex™ autoimmune panel, Thermo Fisher Scientific). Briefly, 2.5µl of serum was incubated with MagPlex microspheres conjugated to 19 multiplexed human autoimmune antigens following the manufacturer's instructions, followed by data acquisition using a Luminex200™ system. Median Fluorescence indices (MFI) were corrected for background signal and non-specific binding using an internal BSA protein control before processing. Differences in autoantibody positivity between patients and controls were assessed (based on the distribution of autoantibody levels in the control population). Subsequently, after determining the optimal clustering algorithm and number of clusters (K), autoantibody samples of patients and controls were clustered using partitioning around medoids with K=3. Only autoantibody samples and not clinical characteristics were included in the clustering to prevent bias. Differences between autoantibody positivity, clinical characteristics, and mortality between clusters were assessed using Chi-square tests, AN(C)OVAs, Kruskal-Wallis tests, and log-rank tests. Full details on the statistical analysis and clustering methods are described in the online supplement.

Additional details on the methodology for detection of BMPR2 autoantibodies, including GST fusion microarray screen, BMPR2 autoantibody ELISA and pulmonary arterial smooth muscle cell culture are provided in the online supplement.

Results

IPAH patients have an immune phenotype defined by a shift in the adaptive immune response axis.

Circulating leukocyte populations were studied by flow cytometry in IPAH patients (n=26, mean age 41.3 ± 10.2 years) selected with no known PAH causing genetic mutations to limit confounding influences of existing pathologies and compared to age and sex matched healthy

donors (n=29). Demographic and clinical characteristics are described in table 1. Antibody staining panels correlated well for lymphocyte gates and major T cell populations across panels (See online supplement Figure E4).

Idiopathic PAH was characterised by a distinct immune profile of altered B cell frequencies, increased circulating T follicular helper cells (cT_{FH}) and an altered regulatory T cell profile (T_{REG}); an immune phenotype indicative of an activated immune response (Figure 1A). We identified significantly enriched populations of plasmablasts (CD3⁻ CD19⁺, CD38⁺, IgD⁻) and double negative B cells (CD3⁻ CD19⁺ CD38⁻ CD27⁻ IgD⁻) and comparative decreases in non-switched memory B cell (CD3⁻ CD19⁺ CD27⁺ IgD⁺) and switched memory B cell (CD3⁻ CD19⁺ CD38⁺ CD27⁺ IgD⁻) frequencies (Figure 1B) in IPAH. A significant increase in ‘circulating’ T_{FH} cells (CD3⁺ CD4⁺ CXCR5⁺ CD45RA⁻ PD1⁺) was observed along with increased levels of T_{REG} (CD3⁺ CD4⁺ CD25⁺ CD127⁻) cells with a comparative reduction in CCR4⁺ primed T_{REG} cells (CD3⁺ CD4⁺ CD25⁺ CD27⁻ CCR4⁺) (Figure 1B). Full results for immunophenotyping can be found in the online supplement table E3. Frequencies of T_{REG} cells correlated with increased frequency of circulating T_{FH} and plasmablasts, and plasmablast levels negatively correlated with non-switched memory B cell frequencies, suggesting an interplay between activity of immune cell sub populations (see online supplement Figure E5).

Immunoglobulin IgG3 and Interleukin 21 are raised in IPAH

Circulating levels of immunoglobulin were subsequently measured in a random subset of IPAH patients with available plasma from the immunophenotyping analysis (n=10). Whilst major subclasses remained unchanged compared to healthy controls (Figure 2A), IgG3 levels were increased in IPAH (q=0.0392, Figure 2B). Interleukin-21 (IL-21) has not been previously measured in IPAH and plays a major role in B cell immunoglobulin response and has been

implicated in the promotion of autoimmune disease (13). IL-21 levels were shown to be significantly increased in IPAHA ($p < 0.0001$, Figure 2C).

Autoantibody levels are increased in IPAHA and HPAHA

Our data is indicative of an aberrant immune phenotype in IPAHA that is suggestive of autoimmune pathology. To assess the prevalence of autoantibodies in PAHA, we utilised the ProtoPlex™ Autoimmune panel to screen for 19 clinically standard and widespread utilised autoantibody biomarkers in sera from a cohort of IPAHA/HPAHA/PVOD/PCH ($n=473$). These were compared to an age and sex propensity-matched healthy donor control cohort ($n=946$) (See Table 2 and online supplementary Table E4 for demographic and clinical characteristics). The analysis plan is summarised in Figure 3 and was devised to: 1) compare PAHA and healthy donor control autoantibody positivity; 2) Identify clusters of patients based on autoantibody profile and 3) stratify clinical outcomes and prognosis based on clustering.

Autoantibody positivity differed significantly between PAHA and healthy donor controls (Figure 4A left hand graphs, online supplement Table E5); 10 autoantibodies differed significantly between groups, of which 9 (Cardiolipin, H2a (F2a2) & H4 (F2a1), La/SS-B antigen, Proteinase-3, RNP complex, Smith-antigen, Thyroglobulin, Thyroid Peroxidase and U1-snRNP 68) were more commonly positive in PAHA (Figure 4B).

Cluster analysis reveals distinct subgroups based upon autoantibody profile

Three distinct clusters based upon autoantibody levels in the combined healthy donor control and PAHA cohorts were identified using partitioning around medoids clustering (PAM), stratifying into a ‘high autoantibody’ cluster, ‘low autoantibody’ cluster, and a small ‘intermediate’ cluster exhibiting high levels of RNP-complex autoantibodies. Stratification of PAHA patients alone resulted in a similar clustering pattern based on autoantibody positivity,

with 27.5% in the ‘high’ cluster (n=130), 61.3% in the ‘low’ cluster (n=290) and 11.2% in the ‘intermediate’ cluster (n=53) (Figure 4A, right hand graphs, Figure 4C heat map and online supplementary Table E6). Subsequent analysis of clusters within PAH patients alone revealed that age at diagnosis and sex distribution were comparable between the clusters (See online supplementary Table E7).

PAH autoantibody clusters have distinct clinical and mortality outcomes.

Comparison of clinical characteristics between PAH patients defined by their autoantibody cluster identified significant differences in haemodynamic parameters (Figure 5, online supplementary Table E7). Pulmonary vascular resistance (PVR) and cardiac output (CO) varied significantly between clusters ($q=0.0063$ and $q=0.018$ respectively) and were worse in the ‘high autoantibody’ cluster (PVR: 14.0 (± 6.5) woods units vs. 11.7 (± 5.4) woods units, 10.8 (± 5.1) woods units; cardiac output: 3.7 (± 1.3) l/min vs 4.1 (± 1.3) l/min, 4.4 (± 1.5) l/min for the ‘high autoantibody’ cluster vs ‘low autoantibody’, ‘intermediate autoantibody’ clusters respectively). No significant differences in pulmonary arterial wedge pressure (PAWP) or mean pulmonary arterial pressure (mPAP) were observed between clusters (Figures 5D,G), nor were any immune mediated co-morbidities or clinical indications of autoimmunity. High and intermediate autoantibody clusters were found to have greater prevalence of co-morbid hypothyroidism (25.4%, 7.9%, 20.8% for the high, low and intermediate clusters respectively), however no differences were identified for thyroid stimulating hormone levels (TSH, $q = 0.20$, Figure 5F). Age and BMI did not impact cluster stratification (Figures 5C & E). No significant differences in treatment were observed between clusters ($q=0.12$). REVEAL risk score did not differ statistically between clusters ($q=0.25$), however, significant variation in WHO functional class was observed between clusters ($q=0.042$); the high autoantibody cluster had a higher proportion of WHO functional class four patients (20.0% vs. 11.3% (low cluster), 1.9%

(intermediate cluster)) and comparatively fewer class three (51.5% (high cluster) vs. 67.6% (low cluster), 71.7% (intermediate cluster). Kaplan-Meier survival curves utilising census data from the patients sampled in the UK National cohort study of Idiopathic and Hereditary PAH differed between clusters (log rank test $p=0.0061$, Figure 5H). This demonstrated improved survival at 20 years post diagnosis between groups and indicating highest survival in the high autoantibody cluster, and after correction for treatment, sex and age at diagnosis in a cox-proportional hazard model (supplemental Figure E6), the low autoantibody cluster remained at a significantly increased risk for mortality (odds ratio: 1.9 (1.17 - 3.0)).

Putative autoantibodies to BMPR2 are detected in IPAH sera

Utilising a candidate-based GST-fusion human proteomic screen we tested the hypothesis that BMPR2 and members of its canonical signalling pathway would represent ‘high value’ targets in an autoantibody immune response in PAH (10). Putative serum autoantibodies against BMPR2 were detected in IPAH patients ($n=5$) and not in patients with other autoimmune aetiologies (SLE, ANCA-associated vasculitis, type 1 diabetes and SSC, $n=11$ Figure 6A). We proceeded to screen 350 IPAH and HPAH patients from the UK National Cohort study of Idiopathic and Heritable PAH and 55 healthy donor controls in a novel ELISA to detect IgG reactivity against a peptide of the extracellular domain (ECD) of human BMPR2. Bound immunoglobulins were significantly increased in PAH patients ($p=0.038$) however they were present in only a small subset of the PAH who exhibited high BMPR2 reactivity (Figure 6B). Whilst samples tested here overlapped with autoantibody biomarker analysis, we identified no significant enrichment into the current autoantibody clusters, though the n is small and this should not be over-interpreted. Pre-incubation of positive sera with BMPR2 ECD prior to incubation in the ELISA demonstrated a dose responsive quenching of signal but with high concentrations for maximal effect (Figure 6C). Functional attenuation of BMP4 signalling in

pulmonary arterial smooth muscle cells was observed with serum pre-treatment from BMPR2 sero-positive patients, compared to serum from healthy controls. Sero-positive samples were shown to significantly reduce the upregulation of *ID1* and *ID3* following BMP4 stimulation indicating a reduction in BMPR2-ALK3 receptor pathway signalling (Figures 6D and 6E).

Discussion

We present data from the largest study to-date to look in-depth at autoimmunity in IPAH. There is clear and consistent evidence across multiple methodologies to suggest that autoimmunity is a clinically important associative feature of IPAH.

The IPAH peripheral blood immune profile was characterised by raised circulating T_{FH} and T_{REG} levels and altered B-cell frequencies. Our observation of increased regulatory T cells reaffirms similar findings in PAH (14), and our observed increases in circulating T_{FH} -like cells are a hallmark of autoimmune disease (15, 16). Raised plasmablasts recapitulate similar works (17), but the findings of increased double negative and decreased memory B cells are novel to IPAH, and likely due in part to the under reporting of B cell populations. Our observed increase in frequency of antibody producing plasmablasts and double negative B cells, and corresponding reduction in memory B cells may indicate a shift in humoral immune axis in our patients in favour of an activated autoimmune state as observed in SLE (18), SSC (19) and Hashimoto's Thyroiditis (20). Raised circulating T_{FH} cells are known to play a role in promoting the differentiation of naïve B-cells into antibody producing plasma cells, inducing secretion of immunoglobulin, and negatively correlate with memory B-cells in various autoimmune diseases (15, 16) and aberrant regulatory T cells demonstrate a loss of control of immune tolerance (21). The finding of raised interleukin 21 in sera provides further weight to immune disruption, as in addition to the well documented rise in IL-6 in PAH which has been linked to prognosis (22), IL-21 has pleiotropic effects on both T-cell and humoral responses.

There is accumulating evidence that high levels result in autoimmune disturbances, giving rise to aberrant levels of T_{FH} , T_{REG} , memory B-cells, plasmablasts, plasma cells and autoantibody production (13) and may be associated with our observation of raised IgG3 (24, 25).

Multiple reports have identified circulating autoantibodies in PAH with some specificity to the vascular environment (17, 26, 27), but this is the first screen of its kind to measure clinically validated and accepted autoantibodies associated with autoimmune disease. Nine autoantibodies were highly significantly increased compared to healthy controls. It is notable that ~40% of our population can be thought to have “positive” autoantibodies using our conservative thresholding across the clusters (with a very small fraction additionally with BMPR2 antibodies). IPAH clustered into three populations with high and low autoantibody prevalence and a smaller ‘intermediate’ subset defined by high anti-RNP complex autoantibodies. The latter cohort is strikingly different in autoantibody profile with 100% of all classified subjects having isolated positivity to the RNP-complex antibody only, and in the absence of the clinical features of related autoimmune diseases. Secondary analysis of patient clusters identified distinctions in haemodynamic characteristics that were defined by autoantibody prevalence, as cardiac output, PVR and WHO classification were worsened in the high autoantibody cluster. Paradoxically, this cluster had improved long-term survival which was unaffected by sex, age and medication. This finding is intriguing, but consistent with previous genetic data in an international GWAS study where an association with specific HLA- DPB1 alleles is a risk factor for developing PAH, but also associated with improved survival outcomes (8) and whole blood transcriptomics that identify HLA gene expression as drivers survival associated endophenotypes (9). This uncoupling of haemodynamics with longer-term outcomes is important and counter to our current understanding of disease progression. The critical questions remains whether autoimmunity/inflammation is a cause of PAH, a response to PAH (for example in response to pulmonary vascular cell damage) or a

confounding variable that modulates response. Irrespective of this question, the demonstration of an HLA locus and now antibody signatures which both associate with better outcomes needs careful consideration. Further work is required to study the effects of patients longitudinally to assess if inflammation/autoimmunity is consistent in a subset of the disease or if it follows a profile of relapsing/remitting. Associations of immune clusters with treatment may need to be re-thought for the purpose of future trials. Recent work by our group failed to demonstrate a treatment effect in a stable group of unstratified PAH patients using the anti-IL-6 drug Tocilizumab based on haemodynamic outcomes (28). Post-hoc findings by Zamanian *et al* (29) utilised machine learning to associate serum levels of rheumatoid factor, IL-12 and IL-17 with the greatest improvement in SSC-PAH patients treated with the anti- CD20 drug, Rituximab in a trial designed to study the effect of B cell depletion on disease pathology and prognosis. Pertinently, the authors acknowledge that the use of molecular phenotyping can identify potential biomarkers to predict the responsiveness of treatments to allow for enrichment for optimal clinical trial patient selection. These current studies directly challenge how targeting inflammation may need a refining from the perspective of who we target and at what point of the disease.

In our final line of enquiry, we examined whether serum from patients contained autoantibodies to the key genetic pathway pivotal in PAH biology; the BMPR2 pathway. Pathogenic anti-endothelial antibodies have been previously described in PAH, but none with affinity to proteins relevant to genetic causes of disease (17, 27). We report on a putative autoantibody to the pathological ‘high value’ target, BMPR2, and evidence of an in-vitro functional response on pulmonary vascular cells with reduced down-stream canonical signalling with BMP ligand stimulation. The possibility of functional autoantibodies directed at key vascular cell pathways is important both pathobiologically and in considering responses to therapies, for example targeting the BMPR2 pathway- Sotatercept being the most advanced and currently in phase 3

studies (30). It is not clear yet how these less-common autoantibodies relate to the clusters we have observed.

In summary, we present the most comprehensive study of autoimmunity in IPAH and demonstrate strong evidence for an association with the disease. Autoimmunity showed association with both haemodynamic parameters and clinical outcomes and the demonstration of autoantibodies to BMPR2 opens up the possibility that autoantibodies are targeting key pathways leading to vascular dysfunction. Studies are required to understand the longitudinal variability and future clinical trials may need to consider autoimmunity and inflammation in stratification techniques.

Acknowledgments: The authors thank all the patients and control volunteers who donated to this research. They also thank the UK National cohort study of Idiopathic and Heritable PAH, their research nurses and coordinators at the specialist pulmonary hypertension centres involved in this study. We would like to acknowledge the NIHR Bioresource and NIHR Cardiorespiratory BRC who supported this work.

References

1. Lai YC, Potoka KC, Champion HC, Mora AL, Gladwin MT. Pulmonary arterial hypertension: The clinical syndrome. *Circulation Research* 2014;115:115–130.
2. Batton KA, Austin CO, Bruno KA, Burger CD, Shapiro BP, Fairweather DL. Sex differences in pulmonary arterial hypertension: Role of infection and autoimmunity in the pathogenesis of disease. *Biology of Sex Differences* 2018;9:1–14.
3. Mouthon L, Guillevin L, Humbert M. Pulmonary arterial hypertension: An autoimmune disease? *European Respiratory Journal* 2005;26:986–988.
4. Savai R, Pullamsetti SS, Kolbe J, Bieniek E, Voswinckel R, Fink L, Scheed A, Ritter C, Dahal BK, Vater A, Klussmann S, Ghofrani HA, Weissmann N, Klepetko W, Banat GA, Seeger W, Grimminger F, Schermuly RT. Immune and inflammatory cell involvement in the pathology of idiopathic pulmonary arterial hypertension. *American Journal of Respiratory and Critical Care Medicine* 2012;186:897–908.
5. Marsh LM, Jandl K, Grünig G, Foris V, Bashir M, Ghanim B, Klepetko W, Olschewski H, Olschewski A, Kwapiszewska G. The inflammatory cell landscape in the lungs of patients with idiopathic pulmonary arterial hypertension. *European Respiratory Journal* 2018;51:1701214.
6. Perros F, Dorfmueller P, Montani D, Hammad H, Waelput W, Girerd B, Raymond N, Mercier O, Mussot S, Cohen-Kaminsky S, Humbert M, Lambrecht BN. Pulmonary lymphoid neogenesis in idiopathic pulmonary arterial hypertension. *American Journal of Respiratory and Critical Care Medicine* 2012;185:311–321.
7. Nicolls MR, Taraseviciene-Stewart L, Rai PR, Badesch DB, Voelkel NF.

- Autoimmunity and pulmonary hypertension: A perspective. *European Respiratory Journal* 2005;26:1110–1118.
8. Rhodes CJ, Batai K, Bleda M, Haimel M, Southgate L, Germain M, Pauciulo MW, Hadinnapola C, Aman J, Girerd B, Arora A, Knight J, Hanscombe KB, Karnes JH, Kaakinen M, Gall H, Ulrich A, Harbaum L, Cebola I, Ferrer J, Lutz K, Swietlik EM, Ahmad F, Amouyel P, Archer SL, Argula R, Austin ED, Badesch D, Bakshi S, *et al.* Genetic determinants of risk in pulmonary arterial hypertension: international genome-wide association studies and meta-analysis. *The Lancet Respiratory Medicine* 2019;7:227–238.
 9. Kariotis S, Jammeh E, Swietlik EM, Pickworth JA, Rhodes CJ, Otero P, Wharton J, Iremonger J, Dunning MJ, Pandya D, Mascarenhas TS, Errington N, Thompson AAR, Romanoski CE, Rischard F, Garcia JGN, Yuan JX-J, An T-HS, Desai AA, Coghlan G, Lordan J, Corris PA, Howard LS, Condliffe R, Kiely DG, Church C, Pepke-Zaba J, Toshner M, Wort S, *et al.* Biological heterogeneity in idiopathic pulmonary arterial hypertension identified through unsupervised transcriptomic profiling of whole blood. *Nature Communications* 2021;12:1–14.
 10. Morrell NW, Adnot S, Archer SL, Dupuis J, Lloyd Jones P, MacLean MR, McMurtry IF, Stenmark KR, Thistlethwaite PA, Weissmann N, Yuan JXJ, Weir EK. Cellular and Molecular Basis of Pulmonary Arterial Hypertension. *Journal of the American College of Cardiology* 2009;54(1 Suppl):S20-S30.
 11. Gräf S, Haimel M, Bleda M, Hadinnapola C, Southgate L, Li W, Hodgson J, Liu B, Salmon RM, Southwood M, Machado RD, Martin JM, Treacy CM, Yates K, Daugherty LC, Shamardina O, Whitehorn D, Holden S, Aldred M, Bogaard HJ, Church C, Coghlan G, Condliffe R, Corris PA, Danesino C, Eyries M, Gall H, Ghio S,

- Ghofrani HA, *et al.* Identification of rare sequence variation underlying heritable pulmonary arterial hypertension. *Nature Communications* 2018;9(1):1416.
12. Maecker H, McCoy JP, Nussenblatt R. Standardizing immunophenotyping for the Human Immunology. *Nat Rev Immunol* 2012;12:191–200.
 13. Long D, Chen Y, Wu H, Zhao M, Lu Q. Clinical significance and immunobiology of IL-21 in autoimmunity. *Journal of Autoimmunity* 2019;99:1–14.
 14. Austin ED, Rock MT, Mosse CA, Vnencak-Jones CL, Yoder SM, Robbins IM, Loyd JE, Meyrick BO. T lymphocyte subset abnormalities in the blood and lung in pulmonary arterial hypertension. *Respiratory Medicine* 2010;104:454–462.
 15. Szabo K, Papp G, Barath S, Gyimesi E, Szanto A, Zeher M. Follicular helper T cells may play an important role in the severity of primary Sjögren’s syndrome. *Clinical Immunology* 2013;147:95–104.
 16. Gensous N, Charrier M, Duluc D, Contin-Bordes C, Truchetet ME, Lazaro E, Duffau P, Blanco P, Richez C. T follicular helper cells in autoimmune disorders. *Frontiers in Immunology* 2018;9:1637.
 17. Blum LK, Cao RRL, Sweatt AJ, Bill M, Lahey LJ, Hsi AC, Lee CS, Kongpachith S, Ju CH, Mao R, Wong HH, Nicolls MR, Zamanian RT, Robinson WH. Circulating plasmablasts are elevated and produce pathogenic anti-endothelial cell autoantibodies in idiopathic pulmonary arterial hypertension. *European Journal of Immunology* 2018;48:874–884.
 18. Jenks SA, Cashman KS, Zumaquero E, Marigorta UM, Patel A V., Wang X, Tomar D, Woodruff MC, Simon Z, Bugrovsky R, Blalock EL, Scharer CD, Tipton CM, Wei C,

- Lim SS, Petri M, Niewold TB, Anolik JH, Gibson G, Lee FEH, Boss JM, Lund FE, Sanz I. Distinct Effector B Cells Induced by Unregulated Toll-like Receptor 7 Contribute to Pathogenic Responses in Systemic Lupus Erythematosus. *Immunity* 2018;49:725-739.e6.
19. Gumkowska-Sroka O, Jagoda K, Owczarek A, Helbig G, Gienza-Stokłosa J, Kotyla PJ. Cytometric Characterization of Main Immunocompetent Cells in Patients with Systemic Sclerosis: Relationship with Disease Activity and Type of Immunosuppressive Treatment. *Journal of Clinical Medicine* 2019;8:625.
20. Liu Y, Gong Y, Qu C, Zhang Y, You R, Yu N, Lu G, Huang Y, Zhang H, Gao Y, Gao Y, Guo X. CD32b expression is down-regulated on double-negative memory B cells in patients with Hashimoto's thyroiditis. *Molecular and Cellular Endocrinology* 2017;440:1–7.
21. Sakaguchi S, Yamaguchi T, Nomura T, Ono M. Regulatory T Cells and Immune Tolerance. *Cell* 2008;133:775–787.
22. Soon E, Holmes AM, Treacy CM, Doughty NJ, Southgate L, MacHado RD, Trembath RC, Jennings S, Barker L, Nicklin P, Walker C, Budd DC, Pepke-Zaba J, Morrell NW. Elevated levels of inflammatory cytokines predict survival in idiopathic and familial pulmonary arterial hypertension. *Circulation* 2010;122:920–927.
23. Jones BE, Maerz MD, Buckner JH. IL-6: a cytokine at the crossroads of autoimmunity. *Current Opinion in Immunology* 2018;55:9–14.
24. Pène J, Gauchat J-F, Lécart S, Drouet E, Guglielmi P, Boulay V, Delwail A, Foster D, Lecron J-C, Yssel H. Cutting Edge: IL-21 Is a Switch Factor for the Production of IgG 1 and IgG 3 by Human B Cells . *The Journal of Immunology* 2004;172:5154–

- 5157.
25. Zhang H, Li P, Wu D, Xu D, Hou Y, Wang Q, Li M, Li Y, Zeng X, Zhang F, Shi Q. Serum IgG subclasses in autoimmune diseases. *Medicine (United States)* 2015;94:e387.
 26. Terrier B, Tamby MC, Camoin L, Guilpain P, Broussard C, Bussone G, Yaïci A, Hotellier F, Simonneau G, Guillevin L, Humbert M, Mouthon L. Identification of target antigens of antifibroblast antibodies in pulmonary arterial hypertension. *American Journal of Respiratory and Critical Care Medicine* 2008;177:1128–1134.
 27. Tamby MC, Chanseaud Y, Humbert M, Fermanian J, Guilpain P, Garcia-De-La-Peña-Lefebvre P, Brunet S, Servettaz A, Weill B, Simonneau G, Guillevin L, Boissier MC, Mouthon L. Anti-endothelial cell antibodies in idiopathic and systemic sclerosis associated pulmonary arterial hypertension. *Thorax* 2005;60:765–772.
 28. Toshner M, Church C, Harbaum L, Rhodes C, Moreschi SSV, Liley J, Jones R, Arora A, Batai K, Desai AA, Coghlan JG, Gibbs JSR, Gor D, Gräf S, Harlow L, Hernandez-sanchez J, Howard LS, Humbert M, Karnes J, Kiely DG, Kittles R, Knightbridge E, Lam B, Lutz KA, Nichols WC, Pauciulo MW, Pepke-zaba J, Suntharalingam J, Soubrier F, *et al.* Early View Mendelian randomisation and experimental medicine approaches to IL-6 as a drug target in PAH. *Eu Respir J* 2021;2002463.
 29. Zamanian RT, Badesch D, Chung L, Domsic RT, Medsger T, Pinckney A, Keyes-Elstein L, D'Aveta C, Spychala M, White RJ, Hassoun PM, Torres F, Sweatt AJ, Molitor JA, Khanna D, Maecker H, Welch B, Goldmuntz E, Nicolls MR, Fischer A, Domsic R, Molitor J, Frech T, Argula R, Berman-Rosenzweig E, Bernstein E, Farber H, Mayes M, Ford H, *et al.* Safety and efficacy of B-cell depletion with rituximab for

the treatment of systemic sclerosis–associated pulmonary arterial hypertension: A multicenter, double-blind, randomized, placebo-controlled trial. *American Journal of Respiratory and Critical Care Medicine* 2021;204:209–221.

30. Humbert M. Sotatercept for the Treatment of Pulmonary Arterial Hypertension. *The New England journal of medicine* 2021;

Table and Figure Legends

Table 1. Characteristics of immune phenotyped IPAH patients and healthy donor controls. Study groups were matched according to age and gender. Data presented as count or mean \pm standard deviation or raw counts.

Table 2. Demographic characteristics of PAH and matched healthy donor control subjects analysed for autoimmunity autoantibody biomarkers. Data presented as count or mean \pm standard deviation or raw counts.

Figure 1. Peripheral immune profile in IPAH is one of an activated immune response. Analysis of circulating leukocytes from PBMC fraction of peripheral whole blood analysed in IPAH (n=26) and healthy donor controls (n=29) by flow cytometry. A) Sunburst plots showing average distribution of B cell, T_{FH} and T_{REG} populations as a percentage of parent population from their respective panels of CD19⁺ B cells, T helper / follicular helper and CD4⁺ T cells in healthy donors and IPAH. NSM: Non switched memory B cell; PD-1: Programmed cell death protein 1. B) Abundance of cell populations for Plasmablasts (CD3⁻ CD19⁺ CD38⁺ IgD⁻); double negative B cells (CD3⁻ CD19⁺ CD38⁻ CD27⁻ IgD⁻); non-switched memory B cells (CD3⁻ CD19⁺ CD27⁺ IgD⁺); switched memory B cells (CD3⁻ CD19⁺ CD38⁺ CD27⁺ IgD⁻); ‘circulating’ T_{FH} cells (CD3⁺ CD4⁺ CXCR5⁺ CD45RA⁻ PD1⁺); T_{REG} (CD3⁺ CD4⁺ CD25⁺ CD127⁻) and CCR4⁺ Primed T_{REG} (CD3⁺ CD4⁺ CD25⁺ CD27⁻ CCR4⁺). Plots show median with interquartile range except for T_{REG} cells which shows mean with standard deviation. To control for multiple hypothesis testing, false discovery rates were estimated using Benjamini and Hochberg on a per panel basis, and resultant q values are presented. We report here as significant tests q<0.05.

Figure 2. Circulating immunoglobulin and interleukin-21 levels in IPAH. Nephelometry of peripheral immunoglobulin classes in IPAH (n=10) and healthy donor controls (n=27) for

A) major immunoglobulin classes, data shown as mean with standard deviation for IgG and IgM and median with interquartile range for IgA, B) IgG subclasses, data shown as mean with standard deviation for IgG1 and IgG3 and median with interquartile range for IgG2 and IgG4. IPAH patients were selected upon availability of plasma samples from the immunophenotyping cohort. To control for multiple hypothesis testing, false discovery rates were estimated using Benjamini and Hochberg for a total of four tests, and resultant q values are presented. We report here as significant tests $q < 0.05$. C) Interleukin-21 levels in IPAH (n=17) and healthy donor controls (n=60). Data shown as median with interquartile range with Mann-Whitney test.

Figure 3. Strategy for the detection of autoantibody biomarkers in PAH and healthy donor controls and subsequent cluster analysis for the evaluation of clinical characteristics in PAH based on autoantibody status.

Figure 4. Autoantibody analysis in PAH. Circulating autoantibodies were assayed using the ProtoPlex Autoimmune panel in 473 PAH patients and 946 age and sex matched healthy controls. A) Autoantibody levels compared in both healthy controls and PAH patients (left side graphs) and between clusters of PAH patients (right side graphs). Positivity was defined as $0.75Q + 2IQR$ of the control population (shown as dashed line set at 1 for the normalised autoantibody level). Box plots the median with IQR (25%, 75%), whiskers represent the end of the boxplot $\pm 1.5 * IQR$. The y-axis represents the scaled autoantibody level which is normalised to have a median of 0 in the control population and positivity threshold of 1. B) Heat map showing autoantibody positivity prevalence as a % in PAH cases and controls. FDR adjusted q values were calculated across 19 tests and indicated as an *. C) Heat map showing autoantibody positivity prevalence between clusters of PAH cases; high, low and intermediate. FDR adjusted q values were calculated across 19 tests and indicated as an * and indicate which AAB are driving the clustering. Note the null hypotheses of no difference between clusters are

not sensible to test because clusters were defined on the basis of observed values. Panels B and C summarise the significance testing results shown in detail in panel A.

Figure 5. Clinical comparison of clusters in PAH. Boxplot comparison of stratification of clinical outcomes in PAH cohort as determined by autoantibody cluster analysis for A) Pulmonary vascular resistance (PVR); B) Cardiac output; C) Age at diagnosis; D) Pulmonary arterial wedge pressure (PAWP); E) Body mass index (BMI); F) Thyroid stimulating hormone (TSH) level; G) Mean pulmonary arterial pressure (mPAP). Box plots represent the median with IQR (25%, 75%), whiskers represent the end of the boxplot $\pm 1.5 \times \text{IQR}$. Statistical analysis was performed on all available values using two-tailed ANOVA with FDR q-values calculated across 178 tests. TSH levels were log-transformed before the ANOVA. H) Kaplan-Meier survival analysis for patients up to 20 years post diagnosis (n=462). Statistical analysis was performed with pairwise log-rank tests with a global log-rank test on 2 degrees of freedom.

Figure 6. Putative antibodies to BMPR2 are present in PAH patient sera. A) Heat map showing reactivity following a GST-fusion human proteomic screen to identify sera reactivity to proteins in the BMPR pathway. Sera from IPAH (n=5) and comparator autoimmune disease patients (T1 DM: Type 1 diabetes mellitus (n=3); AAV: ANCA associated vasculitis (n=3); SLE: systemic lupus erythematosus (n=2); SSc: systemic sclerosis (n=3)) Heat map shows mean reactivity (A.U.) B) Quantitative analysis of IgG reactivity against a recombinant peptide of the BMPR2 extracellular domain (ECD) in sera from IPAH/HPAH patients (n=350) and healthy donors (n=55). Mann-Whitney test performed between controls and PAH groups. C) Quenching of identified sero-positive samples (n=5) with free ECD prior to incubation on ELISA effectively quenches binding at $>1000\text{ng}$. Data are shown as mean with standard deviation and expressed as a percentage of non-quenched serum. D and E) Effect of serum pre-incubation from controls (n=5) or PAH patients with seropositivity to BMPR2 as shown

by ELISA (n=5) on pulmonary arterial smooth muscle cells (PASMC) for 1 hour followed by stimulation with 10ng/ml BMP4 for 1 hour . Relative quantification of downstream *ID1*(D) and *ID3* (E) by qPCR and normalised to *HPRT* and *B2M*

Table 1. Characteristics of immune phenotyped IPAH patients and healthy donor controls. Study groups were matched according to age and gender. Data presented as count or mean \pm standard deviation or raw counts.

	Healthy	IPAH
Number of subjects	29	26
Age at sampling (years)	41.5 \pm 12.5	41.3 \pm 10.2
Male / Female	5/24	5/21
BMI	24.6 \pm 3.6	27.9 \pm 6.1
Number of smokers	1	1
Autoimmune co-morbidities	0	5
Graves' disease	0	4
Hypothyroidism	0	1
Age at diagnosis	NA	34.7 \pm 12.0
WHO classification I/II/III	NA	5/9/12
6 MWD (meters)	NA	464.8 \pm 113.2
Haemodynamics		
mPAP (mmHg)	NA	50.3 \pm 11.8
mRAP (mmHg)	NA	8.2 \pm 3.3
PVR (woods units)	NA	702.6 \pm 334.8
BNP (pg/ml)	NA	387.5 \pm 625.5
PAH targeted treatment		

PDE5	NA	16
ERA	NA	9
Prostanoid	NA	14
CCB	NA	5
Riociguat	NA	1
Diuretic	NA	10

Abbreviations: BMI: Body mass index; 6 MWD: 6-minute walk distance; mPAP: mean pulmonary arterial pressure; mRAP: mean right arterial pressure; PVR: pulmonary vascular resistance; BNP: brain natriuretic peptide; PDE5: phosphodiesterase-5 inhibitors; ERA: endothelin receptor antagonists; CCB: calcium channel blockers; NA: Not applicable.

Table 2. Demographic characteristics of PAH and matched healthy donor control subjects analysed for autoimmunity autoantibody biomarkers. Data presented as count or mean \pm standard deviation or raw counts.

	Healthy	PAH
Number of subjects	946	473
Age at sampling (years)	53.01 (\pm 13.4)	53.05 (\pm 15.6)
Male / Female	282 / 664	141 / 332
BMI*	..	28.84 (\pm 7.0)

*Missing / not available data: BMI n = 24

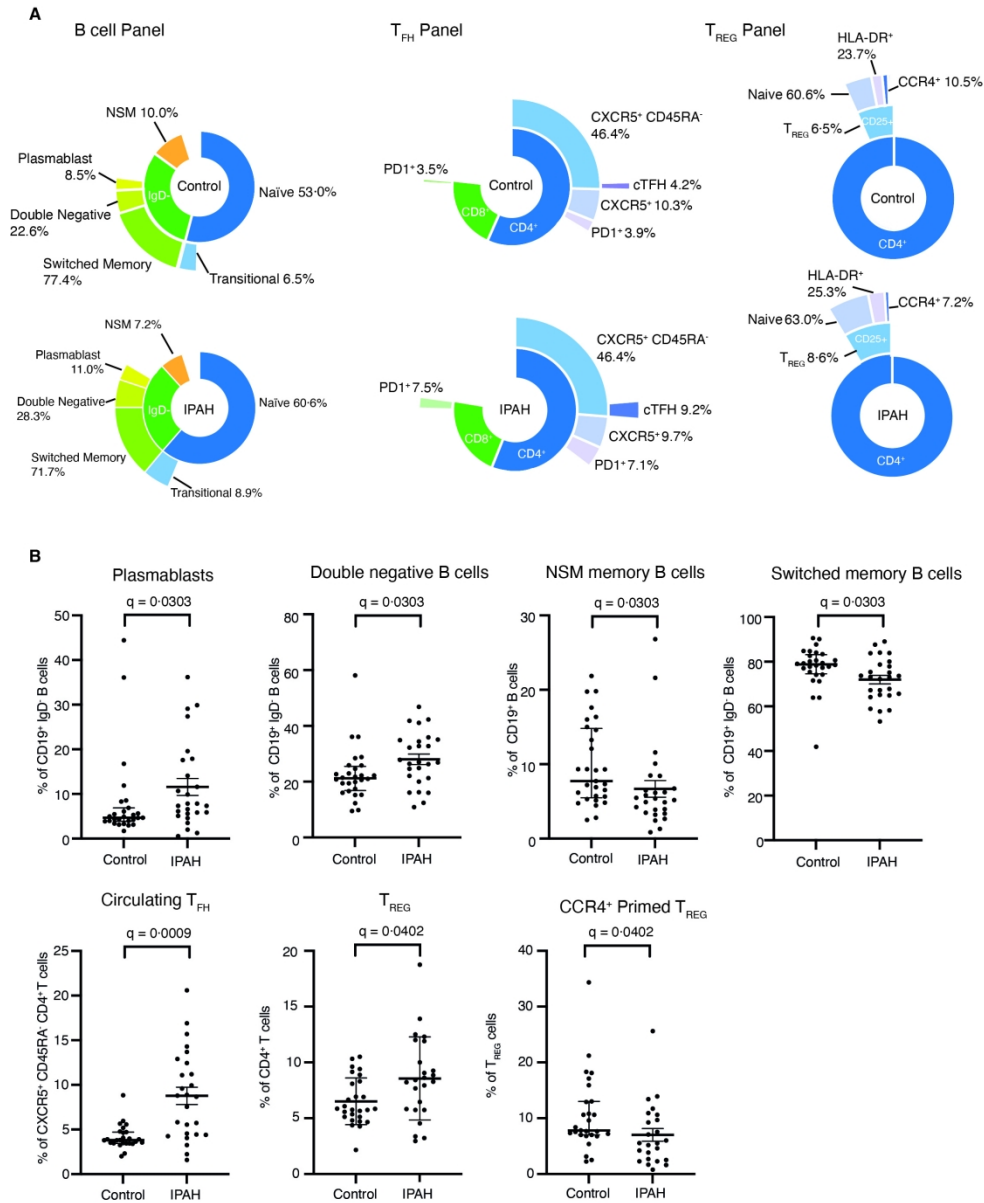


Figure 1. Peripheral immune profile in IPAH is one of an activated immune response.

201x247mm (300 x 300 DPI)

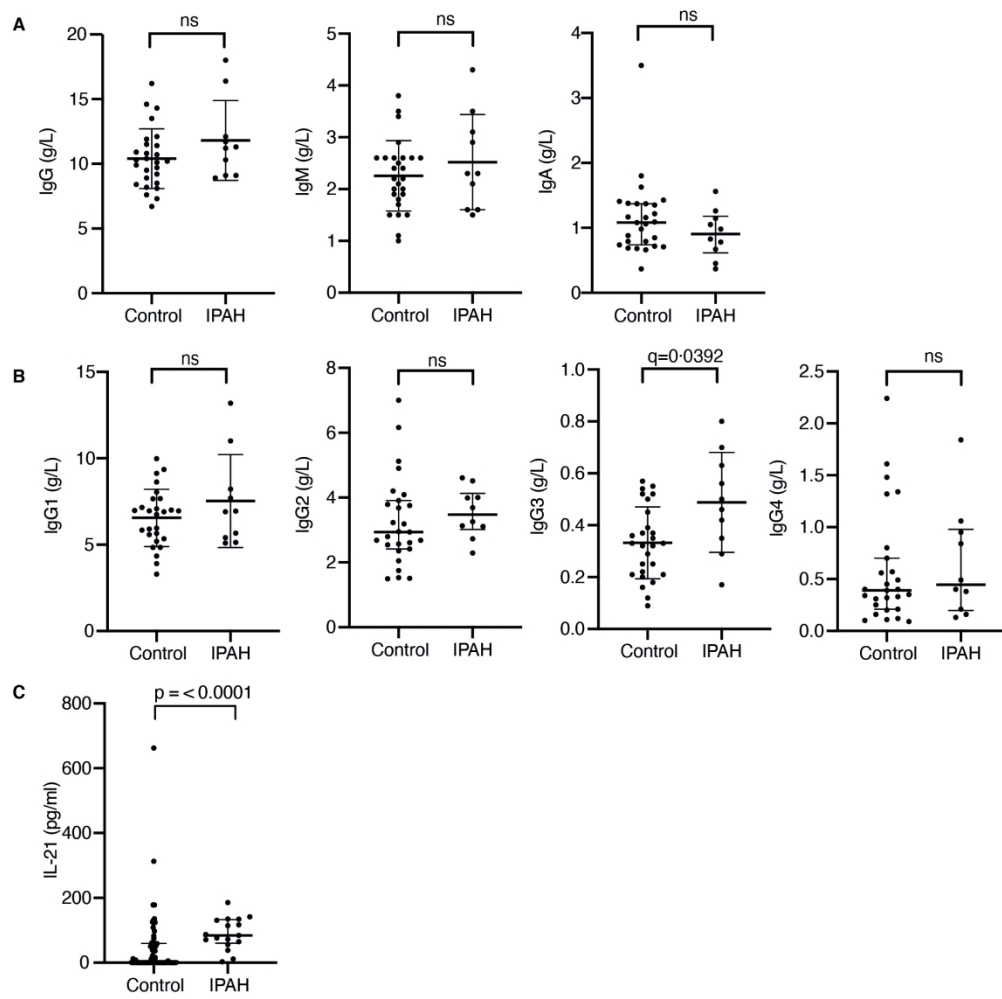


Figure 2. Circulating immunoglobulin and interleukin-21 levels in IPAH.

195x194mm (300 x 300 DPI)

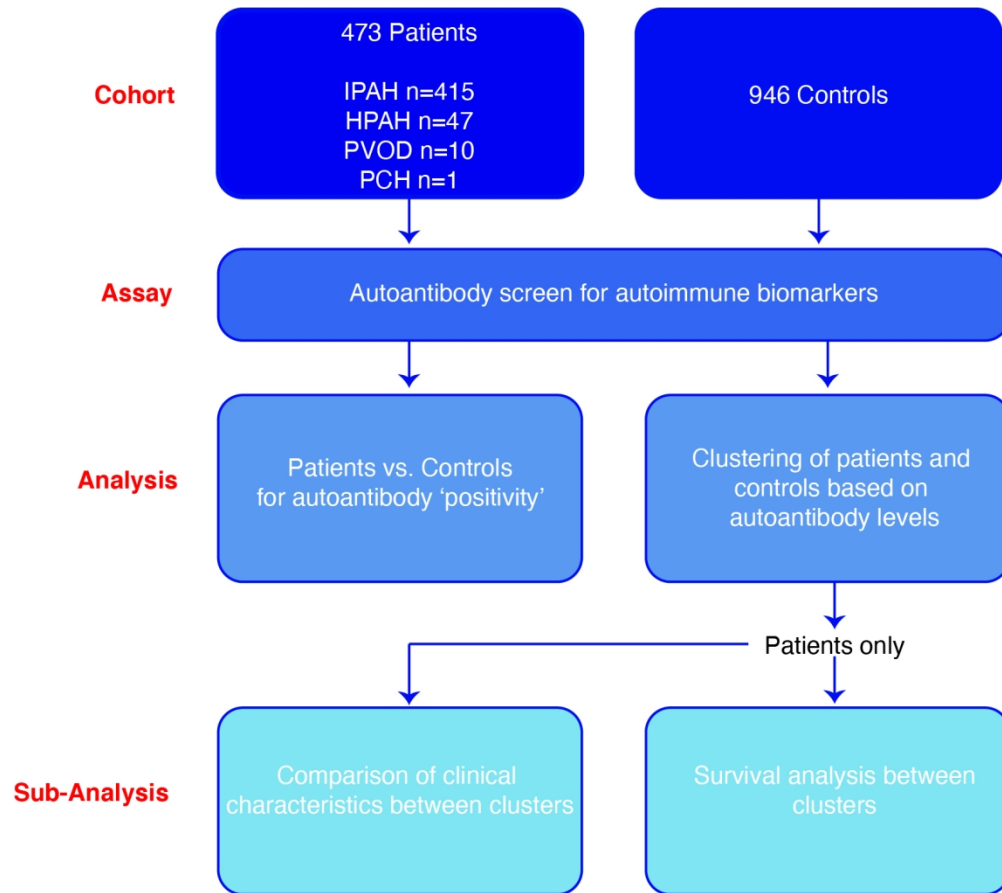


Figure 3. Strategy for the detection of autoantibody biomarkers in PAH and healthy donor controls and subsequent cluster analysis for the evaluation of clinical characteristics in PAH based on autoantibody status.

143x127mm (300 x 300 DPI)

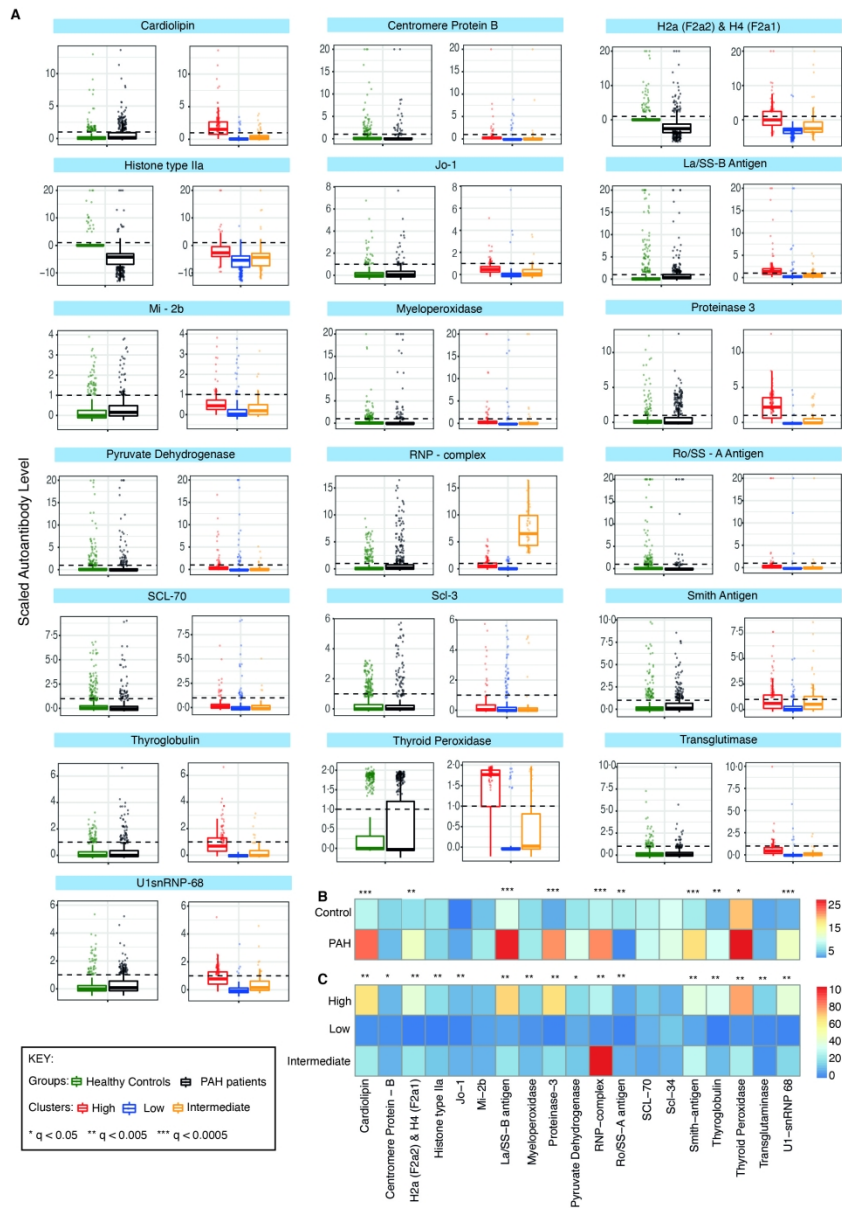


Figure 4. Autoantibody analysis in PAH.

207x296mm (300 x 300 DPI)

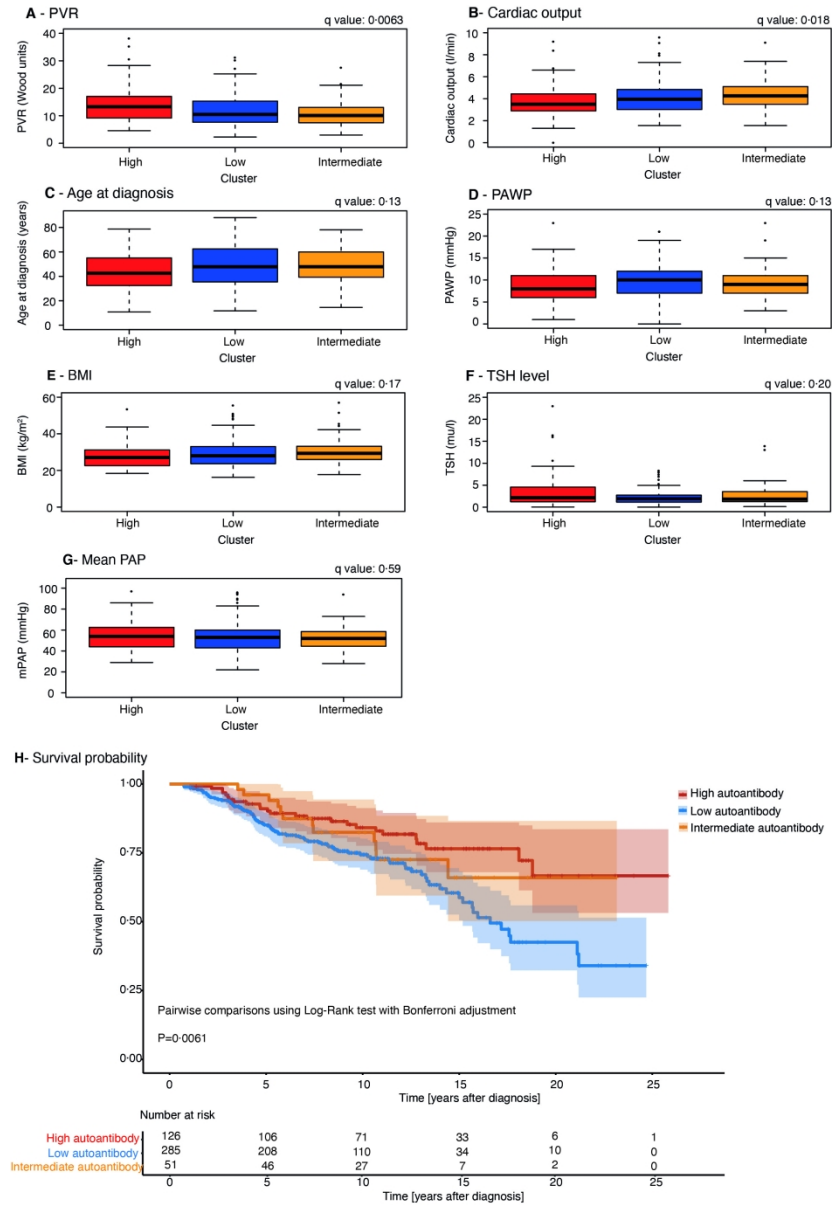


Figure 5. Clinical comparison of clusters in PAH.

200x292mm (300 x 300 DPI)

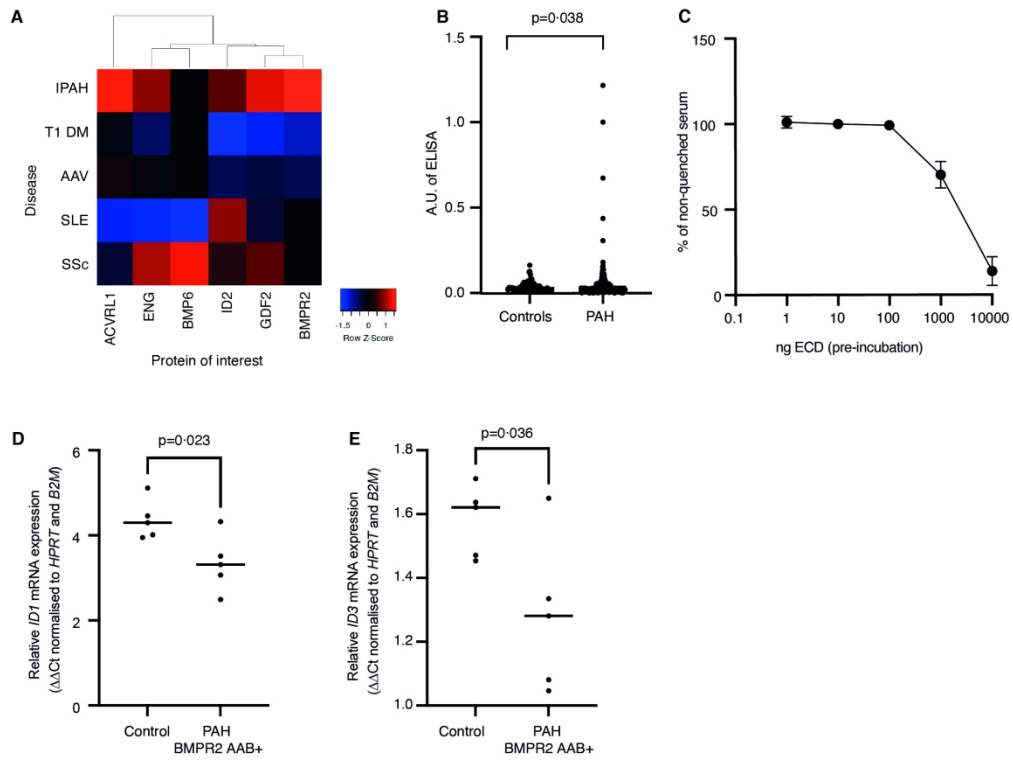


Figure 6. Putative antibodies to BMPR2 are present in PAH patient sera.

198x149mm (300 x 300 DPI)

Online Data Supplement

Autoimmunity is a Significant Feature of Idiopathic Pulmonary Arterial Hypertension

Rowena J. Jones; Eckart M.D.D. De Bie; Emily Groves; Kasia I. Zalewska, Emilia M. Swietlik; Carmen M. Treacy; Jennifer M. Martin; Gary Polwarth; Wei Li; Jingxu Guo; Helen E. Baxendale; Stephen Coleman; Natalia Savinykh; J. Gerry Coghlan; Paul A. Corris; Luke S. Howard; Martin K. Johnson; Colin Church; David G. Kiely; Allan Lawrie; James L. Lordan; Robert V. Mackenzie Ross; Joanna Pepke Zaba; Martin R. Wilkins; S. John Wort; Edoardo Fiorillo; Valeria Orrù; Francesco Cucca; Christopher J. Rhodes; Stefan Gräf; Nicholas W. Morrell; Eoin F. McKinney; Chris Wallace; Mark Toshner

The UK National PAH Cohort Study Consortium

Supplementary Methods

Statistical analysis of flow cytometric standardised immunophenotyping.

Statistical comparisons were performed using GraphPad Prism version 8. Analysis of the detailed immune profiles of patients was performed on frequencies of cell populations represented as a percentage of the parent population. Patient and healthy donor groups were compared using unpaired t-test or Mann-Whitney test based on data normality as determined by D'Agostino & Pearson test for normality. To control for multiple hypothesis testing, false discovery rates were estimated using Benjamini and Hochberg on a per panel basis, and resultant q values are presented. That is, FDR was run separately for the sets of tests displayed within each panel of Figure 1, the whole of Figure 2, Figure 4B, Figure 4C and Figure 5. We report here as significant tests $q < 0.05$. Correlation analysis was performed using two-tailed Pearson correlation co-efficient or Spearman correlation dependent upon normality of the data. Sunburst plots were generated in Microsoft Excel.

Quantification of immunoglobulin levels and interleukin-21

Peripheral blood serum samples were prepared and stored at -80°C prior to analysis. Standard nephelometry was used to determine absolute amounts of immunoglobulin subclasses present in sera. Levels of serum IL-21 were quantified using the Human IL-21 Ready-SET-Go ELISA (eBioscience).

Descriptive statistics of the PAH patients in the autoantibody analysis.

Differences in demographics, haemodynamic parameters and clinical indications for autoimmunity were compared between different PAH aetiologies using ANOVAs and Chi-square tests. A similar comparison was made between incident and prevalent cases, using independent samples T-tests and Chi-square tests. To control for multiple hypothesis testing,

false discovery rates were estimated using Benjamini and Hochberg within each set of 22 tests, and resultant q values are presented. We report here as significant tests $q < 0.05$.

Statistical analysis of autoantibody quantitation assay.

Statistical comparisons were performed using R/R studio v3.6.3 using the stats (v3.6.3) and Publish (v2019.12.04) packages. The base (v3.6.3), MatchIt (v3.0.2), stringdist (v0.9.6.3), data.table (v1.13.0) and tidyverse (v1.3.0) packages were used for data transformations. We report here as significant tests $q < 0.05$. \log_e transformed autoantibody values for 473 patients and 946 healthy donor controls were assessed for autoantibody positivity. A subject was classified as positive for an autoantibody if levels exceeded $0.75Q + 2IQR$ of the control population. Differences in positivity prevalence between cases and controls for each autoantibody were assessed with a Chi-square test and FDR q-values were calculated across 19 tests. Clustering was performed using PAM (partition around medoids) because we considered using medoids more robust to the non-normal distribution of some autoantibodies. Euclidean distances were used, as data was on the same scale and only one type of variable was used. We used silhouette and elbow plots to identify the optimal number of clusters (K) and determined that $K=3$ was optimal for this dataset (See Figure E2). Differences in autoantibody positivity proportions between clusters was assessed with a Chi-square test and FDR q-values were calculated across 19 tests. Differences between clusters of patients alone based on autoantibody levels and clinical data at diagnosis were assessed using Kruskal-Wallis, AN(C)OVA and Chi-square tests and FDR q-values were calculated across 178 tests. Comparison of clinical outcomes with autoantibody clusters was assessed using ANOVA on numeric clinical data (exception; TSH levels were \log_e transformed). Where numeric clinical data differed significantly, an ANCOVA correcting for BMI, age at diagnosis, sex and aetiology was performed with Bonferroni correction for three tests. Survival was assessed using

log-rank tests based on right-censored left-truncated Kaplan-Meier curves with the survival (v3.2-3) and survminer (v0.4.8) packages for 462 patients (only patients with a time to event less than or equal to 20 years were included to reduce immortal time bias). The same packages were used to calculate survival differences (odds ratios), corrected for age at diagnosis, sex and treatment, using a Cox-proportional hazard model. Where FDR adjustment (according to Benjamini & Hochberg) was not possible i.e. for comparisons with ten or less tests, Bonferroni correction was applied. Data was visualised using the ggplot2 (v3.3.0), Pheatmap (v1.0.12), ggbeeswarm (v0.6.0), cowplot (v1.1.0), ggrastr (v0.2.1), Factoextra (v1.0.7), survival (v3.2-3), and survminer (v0.4.7) packages. The complete code used for the analyses of the PAH cohort (n=473) and healthy controls (n=946) in relation to the 19 autoantibodies can be found on: https://github.com/EckartDeBie/Autoimmunity_in_PAH.

Autoantibody microarray discovery

Autoantibody screening was undertaken using a custom protein microarray platform (HuProt™ version 2.0) platform in collaboration with Cambridge Protein Arrays Ltd. (Cambridge, UK). Protein microarrays consisted of a glass microscope slide with a thin SuperEpoxy coating, printed with triplicate spots of recombinant yeast-expressed whole proteins fused with a GST (glutathione-S-transferase) tag. The array included 19,500 targets with selected proteins in the BMPR pathway analysed for this study. Slides were blocked in PBS with 2% BSA /0.1% Tween-20 overnight at 4°C, washed, and then incubated with serum diluted 1:1000 at room temperature for two hours before washing and incubation at room temperature for two hours with fluorophore-conjugated goat anti-human IgM- μ chain-Alexa488 and goat anti-human IgG-Fc-DyLight550 secondary antibodies (Invitrogen). After further washing, slides were scanned using a Tecan LS400 scanner with images extracted using GenePix Pro v4 software. Sera from five patients with IPAHA were included in addition to positive control autoantibody

driven disease samples in type one diabetes mellitus (n=3), ANCA associated vasculitis (n=3), systemic lupus erythematosus (n=2) and scleroderma (n=3).

BMPR2 Autoantibody ELISA

Putative autoantibodies to the extracellular domain (ECD) of BMPR2 were detected using a novel ELISA. BMPR2 ECD was generated as previously described (1). Serum samples were obtained from 350 IPAH/ HPAH patients and 55 healthy donor controls and stored at -80°C prior to analysis. Diluted sera were incubated overnight at 4°C on microplates that had been pre-coated with 100ng of BMPR2 ECD and subsequently exposed to a blocking reagent of PBS with 0.1% Tween-20. Serum dilution of 1:250 in PBS with 0.05% Tween-20 was initially determined (See online supplementary Figure E3A). Immunoglobulin bound to the ECD was detected using Horseradish peroxidase-conjugated anti human IgG monoclonal antibody (Invitrogen) and quantified by addition of Tetramethylbenzidine which was terminated with addition of 1M H₂PO₄ and measured at 450nm (550nm subtraction, BioRad). The results of the tested samples were normalised against a positive reference serum. All samples were tested in duplicate and coefficient of variation of inter-assay variability was tested (See online supplementary Figure E3B). To check for false positivity, IgG reactive sera were incubated in the absence of coated ECD and if still shown to be reactive were removed from the analysis (See online supplementary Figure E3C). To test the ability of free ECD to quench sera immunoglobulins from binding bound peptide, a range of 1 to 10,000 ng ECD was preincubated overnight at 4°C with sera that had demonstrated reactivity to BMPR2 ECD and then subjected to the ELISA assay.

Pulmonary arterial smooth muscle cell treatment with serum

Pulmonary arterial smooth muscle cells from healthy donors were cultured in DMEM (Thermo Fisher) with 10% FBS (Thermo Fisher) and antibiotics / antimetabolites (Thermo Fisher) in 12

well plates until 80% confluence. Cells were serum starved overnight in DMEM plus 0.1% FBS. Cells were subsequently pre-incubated for one hour in 0.1% FBS DMEM with a 1 in 100 dilution of serum from either PAH patients showing BMP2 sero-positivity in the BMP2 ELISA (n=5), or age and sex matched healthy controls (n=5). The media was then spiked with 10ng/ml BMP4 (RnD Systems) for a further one hour. Cells were then lysed in RLT buffer (Qiagen) containing 1% beta mercaptoethanol (Sigma Aldrich). RNA was extracted using the Qiagen RNease mini kit with on-column DNase digestion. RNA was then quantified using a Nanodrop Lite (Thermo Fisher) and cDNA generated using the High-Capacity cDNA reverse transcription kit (Thermo Fisher) according to manufacturer's instructions. qPCR was then performed using primers for *ID1* (Qiagen Quantitect QT00230650), *ID3* (Qiagen Quantitect QT01673336), *B2M* (F: CTCGCGCTACTCTCTCTTTCT, R: CATTCTCTGCTGGATGACGTG) and *HPRT* (F: GCTATAAATTCTTTGCTGACCTGCTG, R: AATACTTTTATGTCCCCTGTTGACTG). Sybr Green PCR master mix (Thermo) and Rox (Thermo) were used in the reaction, to a final volume of 10ul. Thermal cycling conditions were according to the Sybr Green PCR master mix manufacturer's instructions. Gene expression was determined by the ddCT method and normalised to the average of *B2M* and *HPRT* housekeeping genes. All gene expression is shown as relative expression with BMP4 stimulation compared to unstimulated for that serum treatment.

Supplement References

E1. Jiang H, Salmon RM, Upton PD, Wei Z, Lawera A, Davenport AP, Morrell NW, Li W. The prodomain-bound form of bone morphogenetic protein 10 is biologically active on endothelial cells. *Journal of Biological Chemistry* 2016;291:2954–2966.

Supplementary Methods Tables and Figures

Table E1. Antibody cell surface markers used in immunophenotyping flow cytometry

analysis. Panels are as follows; 1: Myeloid; 2: B cells; 3: Broad T cells; 4: T helper /

follicular helper cells; 5: Regulatory T cells.

Antigen	Fluorochrome	Clone	Isotype	Supplier	Dilution	Panel
CD3	eVolve 605	OKT3	Mouse [IgG2a, κ]	eBioscience	20	1, 2, 3, 4, 5
CD11c	PE/Vio770	MJ4-27G12	Mouse [IgG2b, κ]	Miltenyi	11	1
CD14	eVolve 605	61D3	Mouse [IgG1, κ]	eBioscience	20	1
CD16	APC	CB16	Mouse [IgG1, κ]	eBioscience	20	1
CD19	APC/eFluor780	HIB19	Mouse [IgG1, κ]	eBioscience	20	1
CD20	APC/eFluor780	2H7	Mouse [IgG2b, κ]	eBioscience	20	1, 2
CD56	FITC	MEM188	Mouse [IgG2a, κ]	eBioscience	20	1
CD123	PerCP/Cy5.5	6H6	Mouse [IgG1, κ]	eBioscience	20	1
HLA-DR	eFluor450	L243	Mouse [IgG2a, κ]	eBioscience	20	1, 5
CD19	Brilliant Violet 450	HIB19	Mouse [IgG1, κ]	BD Biosciences	20	2
CD24	PerCP/Cy5.5	ML5	Mouse [IgG2a, κ]	BD Biosciences	20	2
CD27	PE/Cy7	O323	Mouse [IgG1, κ]	eBioscience	20	2
CD38	APC	HIT2	Mouse [IgG1, κ]	BD Biosciences	5	2
IgD	FITC	IA6-2	Mouse [IgG2a, κ]	BD Biosciences	5	2
CCR7	PE	150503	Mouse [IgG2a]	BD Biosciences	5	3
CCR6	PE/Cy7	G034E3	Mouse [IgG2b, κ]	Biolegend	5	3, 4
CD4	APC/eFluor 780	RPA-T4	Mouse [IgG1, κ]	eBioscience	20	3, 4, 5
CD8	eVolve 655	RPA-T8	Mouse [IgG1, κ]	eBioscience	20	3, 4
CD45RA	PerCP/Cy5.5	HI100	Mouse [IgG2b, κ]	eBioscience	20	3, 4, 5
CXCR3	FITC	49801	Mouse [IgG1, κ]	R&D Systems	20	4
CXCR5	PE	51505	Mouse [IgG2b, κ]	R&D Systems	10	4
PD1	APC	J105	Mouse [IgG1, κ]	eBioscience	20	4
CCR4	PE/Vio770	REA279	Human [IgG1]	Miltenyi	11	5
CD25	PE	M-A251	Mouse [IgG1, κ]	BD Biosciences	5	5
CD127	Alexa Fluor 647	HIL-7R-M21	Mouse [IgG1, κ]	BD Biosciences	5	5

Table E2: Antibody cell surface markers panels used in immunophenotyping flow cytometry. Immunophenotyping of PBMCs was performed in panels. FSC: Forward scatter; SSC: Side scatter; PD-1: Programmed cell death protein-1.

Cell Population	FSC	SSC	Cell surface markers							Panel
Myeloid										
Monocytes	Low/Mid	Low/Mid	CD3 ⁻	CD19/20 ⁻	CD14 ⁺					1
Classical Monocyte	Low/Mid	Low/Mid	CD3 ⁻	CD19/20 ⁻	CD14 ⁺	CD16 ⁻				1
Non - Classical Monocyte	Low/Mid	Low/Mid	CD3 ⁻	CD19/20 ⁻	CD14 ⁺	CD16 ⁺				1
Natural killer	Low/Mid	Low/Mid	CD3 ⁻	CD19/20 ⁻	CD14 ⁻	CD56 ⁺				1
Dendritic cells (DCs)	Low/Mid	Low/Mid	CD3 ⁻	CD19/20 ⁻	CD14 ⁻	CD56 ⁻	HLA-DR ⁺			1
Plasmacytoid DCs	Low/Mid	Low/Mid	CD3 ⁻	CD19/20 ⁻	CD14 ⁻	CD56 ⁻	HLA-DR ⁺	CD123 ⁺	CD11c ⁻	1
Myeloid DCs	Low/Mid	Low/Mid	CD3 ⁻	CD19/20 ⁻	CD14 ⁻	CD56 ⁻	HLA-DR ⁺	CD123 ⁻	CD11c ⁺	1
Lymphocytes										
B cells										
B cells	Low	Low	CD3 ⁻	CD19 ⁺						2
Naïve B cells	Low	Low	CD3 ⁻	CD19 ⁺	IgD ⁺⁺	CD27 ⁻				2
Non-switched memory B cells	Low	Low	CD3 ⁻	CD19 ⁺	IgD ⁺	CD27 ⁺				2
Transitional B cells	Low	Low	CD3 ⁻	CD19 ⁺	IgD ⁺⁺	CD24 ⁺	CD38 ⁺			2
Plasmablasts	Low	Low	CD3 ⁻	CD19 ⁺	IgD ⁻	CD38 ⁺⁺				2
Switched memory B cells	Low	Low	CD3 ⁻	CD19 ⁺	IgD ⁻	CD38 ⁺	CD27 ⁺			2
Double negative B cells	Low	Low	CD3 ⁻	CD19 ⁺	IgD ⁻	CD38 ⁻	CD27 ⁻			2
Broad T cells										
CD3 ⁺ T cells	Low	Low	CD3 ⁺							3
CD4 ⁺ T cells	Low	Low	CD3 ⁺	CD4 ⁺	CD8 ⁻					3
CD8 ⁺ T cells	Low	Low	CD3 ⁺	CD8 ⁺	CD4 ⁻					3
CD4 ⁺ Naïve	Low	Low	CD3 ⁺	CD4 ⁺	CD8 ⁻	CD45RA ⁺	CCR7 ⁺			3
CD4 ⁺ Effector memory	Low	Low	CD3 ⁺	CD4 ⁺	CD8 ⁻	CD45RA ⁻	CCR7 ⁻			3
CD4 ⁺ Effector	Low	Low	CD3 ⁺	CD4 ⁺	CD8 ⁻	CD45RA ⁺	CCR7 ⁻			3
CD4 ⁺ Central Memory	Low	Low	CD3 ⁺	CD4 ⁺	CD8 ⁻	CD45RA ⁻	CCR7 ⁺			3

CD8 ⁺ Naïve	Low	Low	CD3 ⁺	CD8 ⁺	CD4 ⁻	CD45RA ⁺	CCR7 ⁺			3
CD8 ⁺ Effector memory	Low	Low	CD3 ⁺	CD8 ⁺	CD4 ⁻	CD45RA ⁻	CCR7 ⁻			3
CD8 ⁺ Effector	Low	Low	CD3 ⁺	CD8 ⁺	CD4 ⁻	CD45RA ⁺	CCR7 ⁻			3
CD8 ⁺ Central memory	Low	Low	CD3 ⁺	CD8 ⁺	CD4 ⁻	CD45RA ⁻	CCR7 ⁺			3
T helper / follicular helper cells										4
T _H 1	Low	Low	CD3 ⁺	CD4 ⁺	CD8 ⁻	CXCR3 ⁺	CCR6 ⁻			4
T _H 2	Low	Low	CD3 ⁺	CD4 ⁺	CD8 ⁻	CXCR3 ⁻	CCR6 ⁻			4
T _H 17	Low	Low	CD3 ⁺	CD4 ⁺	CD8 ⁻	CXCR3 ⁻	CCR6 ⁺			4
T _H 1,17	Low	Low	CD3 ⁺	CD4 ⁺	CD8 ⁻	CXCR3 ⁺	CCR6 ⁺			4
CD4 ⁺ PD-1 ⁺	Low	Low	CD3 ⁺	CD4 ⁺	CD8 ⁻	PD-1 ⁺				4
CD8 ⁺ PD-1 ⁺	Low	Low	CD3 ⁺	CD8 ⁺	CD4 ⁻	PD-1 ⁺				4
Circulating T _{FH}	Low	Low	CD3 ⁺	CD4 ⁺	CD8 ⁻	CXCR5 ⁺	CD45RA ⁻	PD-1 ⁺		4
CD4 ⁺ CXCR5 ⁺	Low	Low	CD3 ⁺	CD4 ⁺	CXCR5 ⁺					4
CD8 ⁺ CXCR5 ⁺	Low	Low	CD3 ⁺	CD8 ⁺	CXCR5 ⁺					4
Regulatory T cell										
T _{REG}	Low	Low	CD3 ⁺	CD4 ⁺	CD25 ⁺	CD127 ⁻				5
CCR4 ⁺ T _{REG}	Low	Low	CD3 ⁺	CD4 ⁺	CD25 ⁺	CD127 ⁻	CCR4 ⁺			5
Naïve T _{REG}	Low	Low	CD3 ⁺	CD4 ⁺	CD25 ⁺	CD127 ⁻	CD45RA ⁻			5
HLA-DR T _{REG}	Low	Low	CD3 ⁺	CD4 ⁺	CD25 ⁺	CD127 ⁻	HLA-DR ⁺			5

Supplementary Methods Figures – Legends

Figure E1: Overview of gating strategy used in immunophenotyping. Peripheral blood mononuclear cells (PBMCs) were first gated according to forward scatter (FSC) and side scatter (SSC) in order to identify cell populations. Cells were then gated for singlets and live cells (LIVE/DEAD). Antibody panels were used for the detection of sub-populations as follows: Broad T cell populations; regulatory T cell populations; helper and follicular helper T cells; B cells and myeloid cells. Boxed areas represent population subsets. HLA-DR: human leukocyte antigen – DR isotype; PD-1: programmed cell death protein – 1.

Figure E2: Assessment of optimal number of clusters for autoantibody clustering. A) Silhouette plot; B) Elbow plot of Log_e transformed autoantibody levels for PAM clustering with Euclidean distances. The silhouette plot and elbow plot indicate the optimal number of clusters (K) for PAM clustering with Euclidean distances. In A) the best performance is seen for $K = 2$, with $K = 3$ being a close second. In B) the first bend in the plot is seen at $K = 3$ with another at $K = 5$. The combination of these results suggests that $K = 3$ is the optimal choice for clustering, which fits with clinical expectations.

Figure E3: Development of a novel ELISA for the detection of autoantibodies to the BMPR2 extracellular domain (ECD). A) Serum from a healthy donor and a PAH patient demonstrating IgG reactivity was titrated to determine optimal sample dilution. B) Co-efficient of variation of two PAH samples shows good inter-plate variation, co-efficient of variation shown as % CV. C) Examples of test for non-specific binding of patient serum demonstrating IgG reactivity to the BMPR2 ECD. Samples were incubated both in the presence and absence of ECD and calculated as percentage binding. Sera with high levels of non-specific absorbance were removed.

Supplementary Results Tables

Supplementary Table E3: Frequencies of peripheral immune cell subsets from patients with IPAH and healthy donor controls as determined by flow cytometry. Data shown as percentage of parent gate, either mean \pm standard deviation (*) with unpaired t-test or median [IQR 25,75%] with Mann Whitney non-parametric t-test (#) dependent on data normality as defined by D'Agostino & Pearson test for IPAH (n=26) and healthy donor controls (n=29). To control for multiple hypothesis testing, false discovery rates were estimated using Benjamini and Hochberg procedure on a per panel basis, and resultant q values are presented. We report here significant tests $q < 0.05$. Lymphocyte, CD3⁺ T cells, CD4⁺ T cells and CD8⁺ T cells averaged across multiple panels. DC: Dendritic cells; PD-1: programmed cell death protein-1; HLA-DR: Human leukocyte antigen-DR isotype.

Phenotypic Markers	Population	Healthy Control (%)	IPAH (%)	p-value	FDR adjusted q-value
Myeloid panel					
CD3 ⁻ , CD19/20 ⁻ , CD14 ⁺	Monocytes*	50.31 (\pm 15.30)	53.85 (\pm 15.90)	0.409	0.617
CD16 ⁻ Monocytes	Monocytes – Classical [#]	94.90 [89.28, 96.58]	94.65 [91.90, 97.05]	0.372	0.617
CD16 ⁺ Monocyte	Monocytes – Non-classical [#]	4.27 [2.34, 9.10]	3.91 [2.00, 5.74]	0.441	0.617
CD3 ⁻ , CD19/20 ⁻ , CD14 ⁻ , CD56 ⁻ , HLA-DR ⁺	Dendritic cells*	26.52 (\pm 12.84)	32.18 (\pm 16.65)	0.165	0.577
CD123 ⁺ , CD11c ⁻ DC's	Plasmacytoid DC*	11.71 (\pm 9.36)	7.51 (\pm 5.12)	0.051	0.355

CD11c ⁺ , CD123 ⁻ DC's	Myeloid DC [#]	21.10 [18.73, 23.00]	20.00 [13.50, 34.85]	0.800	0.800
CD3 ⁻ , CD19/20 ⁻ , CD14 ⁻ , CD56 ⁺	Natural Killer cells*	16.06 (±9.58)	18.02 (±13.66)	0.538	0.628
Lymphocytes* (average)		53.12 (±16.61)	40.46 (±17.15)	0.0075	0.09
B cell panel					
CD3 ⁻ , CD19 ⁺	B cells [#]	2.01 [1.25, 3.27]	2.63 [1.64, 3.98]	0.093	0.108
CD27 ⁻ , IgD ⁺ B cells	Naïve B cells*	54.09 (±13.22)	61.21 (±14.98)	0.067	0.093
CD24 ⁺ , CD38 ⁺ , naïve B cells	Transitional B cells [#]	6.94 [5.65, 7.88]	5.89 [3.94, 10.47]	0.885	0.885
CD27 ⁺ , IgD ⁺ B cells	Non-switched memory B cells [#]	7.74 [5.49, 14.80]	5.29 [3.45, 7.16]	0.0065	0.0303
CD38 ⁺ , CD20 ⁻ , IgD ⁻ B cells	Plasmablasts [#]	4.69 [3.88, 6.90]	7.60 [5.47, 17.68]	0.017	0.0303
CD27 ⁺ , IgD ⁻ B cells	Switched memory B cells [#]	78.78 [74.50, 83.16]	73.03 [65.05, 79.03]	0.015	0.0303
CD38 ⁻ , CD27 ⁻ IgD ⁻ B cells	Double Negative B cells [#]	21.23 [16.84, 25.50]	26.98 [20.98, 34.95]	0.015	0.0303
T cell panel					
T cells (all averaged)					
CD3 ⁺	T Cells*	66.16 (±10.63)	59.80 (±12.97)	0.051	0.305
CD4 ⁺ T cells	CD4 ⁺ T cells [#]	57.20 [47.65, 62.00]	54.05 [28.58, 54.05]	0.818	0.818
CD8 ⁺ T cells	CD8 ⁺ T cells*	22.15 (±7.91)	23.39 (±8.26)	0.573	0.726

CD4⁺ subsets					
CD45RA ⁺ , CCR7 ⁺ , CD4 ⁺ T cells	Naïve*	48.43 (±13.03)	46.44 (±16.60)	0.635	0.726
CD45RA ⁻ , CCR7 ⁺ , CD4 ⁺ T cells	Central Memory*	27.45 (±12.48)	26.06 (±10.04)	0.665	0.726
CD45RA ⁻ , CCR7 ⁻ , CD4 ⁺ T cells	Effector Memory*	18.95 (±6.30)	23.19 (±11.54)	0.108	0.430
CD45RA ⁺ , CCR7 ⁻ , CD4 ⁺ T cells	Effector [#]	1.89 [1.22, 2.77]	2.39 [1.15, 4.62]	0.474	0.712
CD8⁺ subsets					
CD45RA ⁺ , CCR7 ⁺ , CD8 ⁺ T cells	Naïve*	36.51 (±16.67)	32.74 (±18.79)	0.451	0.712
CD45RA ⁻ , CCR7 ⁺ , CD8 ⁺ T cells	Central Memory [#]	7.03 [4.08, 14.09]	5.39 [3.79, 8.23]	0.187	0.464
CD45RA ⁻ , CCR7 ⁻ , CD8 ⁺ T cells	Effector Memory*	33.40 (±15.32)	39.69 (±19.65)	0.207	0.464
CD45RA ⁺ , CCR7 ⁻ , CD8 ⁺ T cells	Effector [#]	10.80 [5.50, 23.88]	17.60 [10.44, 31.35]	0.232	0.464
T Helper / Follicular helper panel					
CCR6 ⁻ , CXCR3 ⁺ , CD4 ⁺ T cells	T _H 1*	16.98 (±9.67)	18.34 (±8.39)	0.584	0.702
CCR6 ⁻ , CXCR3 ⁻ , CD4 ⁺ T cells	T _H 2*	24.76 (±10.02)	29.73 (±10.94)	0.088	0.193
CCR6 ⁺ , CXCR3 ⁻ , CD4 ⁺ T cells	T _H 17*	41.66 (±13.21)	36.75 (±7.91)	0.107	0.193
CCR6 ⁺ , CXCR3 ⁺ , CD4 ⁺ T cells	T _H 1,17 [#]	15.40 [9.15, 23.00]	12.50 [9.93, 21.43]	0.683	0.702
T follicular helper cells					

PD1 ⁺ , CXCR5 ⁺ , CD45RA ⁻ , CD4 ⁺ T cells	Circulating T _{FH} [#]	3.82 [3.46, 4.73]	8.75 [4.43, 12.56]	<0.0001	0.0009
CXCR5 ⁺ , CD4 ⁺ , T cells	CXCR5 ⁺ CD4 ⁺ [#]	10.09 [6.04, 13.73]	9.51 [7.23, 11.51]	0.702	0.702
CXCR5 ⁺ , CD8 ⁺ T cells	CXCR5 ⁺ CD8 ⁺ [#]	0.95 [0.56, 1.70]	0.80 [0.54, 1.44]	0.568	0.702
PD1⁺ T Cells					
PD1 ⁺ CD4 ⁺ T cells	CD4 ⁺ PD1 ⁺ [#]	4.07 [2.95, 4.90]	4.79 [3.21, 8.46]	0.103	0.193
PD1 ⁺ CD8 ⁺ T cells	CD8 ⁺ PD1 ⁺ [#]	3.51 [3.15, 3.88]	4.57 [3.04, 7.22]	0.037	0.168
Regulatory T cell panel					
CD25 ⁺ , CD127 ⁻ , CD4 ⁺ T cells	T _{REG} [*]	6.51 (±2.10)	8.57 (±3.73)	0.018	0.0402
CD45RA ⁻ T _{REG} cells	Naïve T _{REG} [#]	62.10 [53.80, 72.70]	66.20 [58.53, 71.73]	0.300	0.400
CCR4 ⁺ T _{REG} cells	CCR4 ⁺ Primed T _{REG} [#]	7.81 [7.01, 13.00]	5.53 [2.56, 10.37]	0.020	0.0402
HLA-DR ⁺ T _{REG} cells	HLA-DR Activated T _{REG} [#]	23.60 [15.20, 29.60]	24.48 [16.23, 31.88]	0.546	0.546

Supplementary Table E4. Clinical characteristics of PAH and healthy donor control subjects analysed for autoimmunity autoantibody biomarkers. Numeric data reported as mean \pm standard deviation and count data are reported as count (percentage per group). Differences between groups were assessed with chi-square tests and ANOVAs for the PAH subtypes and chi-square tests and independent T-test for case status. To control for multiple hypothesis testing, false discovery rates were estimated using the Benjamini and Hochberg procedure within each set of 22 tests, and resultant q values are presented. We report here as significant tests $q < 0.05$. Additional comorbid autoimmune diseases assessed for but not detected: SLE, systemic sclerosis, undifferentiated connective tissue disease, necrotising vasculopathies and overlap syndrome.

Supplementary Table E4

		HPAH (n=47)	IPAH (n=415)	PCH (n=1)	PVOD (n=10)	Total (n=473)	p-value	FDR- adjusted q- value	Incident (n=135)	Prevalent (n=334)	Total (n=469)	p-value	FDR- adjusted q- value
Demographics													
Sex	Female	33 (70.2%)	292 (70.4%)	0 (0.0%)	7 (70.0%)	332 (70.2%)	0.50	0.99	81 (60.0%)	248 (74.3%)	329 (70.1%)	0.0033	0.018
	Male	14 (29.8%)	123 (29.6%)	1 (100.0%)	3 (30.0%)	141 (29.8%)			54 (40.0%)	86 (25.7%)	140 (29.9%)		
Case status*	Incident	14 (29.8%)	110 (26.8%)	1 (100.0%)	10 (100.0%)	135 (28.8%)	3.53e-6	2.47e-5					
	Prevalent	33 (70.2%)	301 (73.2%)	0 (0.0%)	0 (0.0%)	334 (71.2%)							
PAH status	HPAH								14 (10.4%)	33 (9.9%)	47 (10.0%)	3.53e-6	3.71e-5
	IPAH								110 (81.5%)	301 (90.1%)	411 (87.6%)		
	PCH								1 (0.7%)	0 (0.0%)	1 (0.2%)		
	PVOD								10 (7.4%)	0 (0.0%)	10 (2.1%)		
Haemodynamic parameters													
PAWP* (mmHg)		8.7 (±3.6)	9.3 (±3.9)	6	10.3 (±2.5)	9.3 (3±.8)	0.52	0.99	8.6 (±3.3)	9.6 (±4.0)	9.3 (±3.8)	0.013	0.055
PVR* (Wood Units)		15.7 (±7.0)	11.9 (±5.6)	5	10 (±3.8)	12.2 (±5.8)	3.3e-4	0.0017	12 (±5.5)	12.3 (±5.9)	12.2 (±5.8)	0.63	0.75
mPAP* (mmHg)		56.5 (±13)	53 (±13.1)	25	48.8 (±12.2)	53.2 (±13.1)	0.032	0.13	50.4 (±12.6)	54.3 (±13.2)	53.2 (±13.1)	0.0040	0.018
Risk scores and functional status													
REVEAL risk score*	Very high risk	6 (12.8%)	8 (1.9%)	0 (0.0%)	6 (60.0%)	20 (4.2%)	2.20e-16	4.62e-15	12 (8.9%)	8 (2.4%)	20 (4.3%)	3.56e-7	7.47e-6
	High risk	12 (25.5%)	51 (12.3%)	0 (0.0%)	2 (20.0%)	65 (13.7%)			28 (20.7%)	37 (11.1%)	65 (13.9%)		
	Moderate risk	14 (29.8%)	51 (12.3%)	0 (0.0%)	2 (20.0%)	67 (14.2%)			31 (23.0%)	36 (10.8%)	67 (14.3%)		
	Low risk	5 (10.6%)	197 (47.5%)	1 (100.0%)	0 (0.0%)	203 (42.9%)			39 (28.9%)	164 (49.1%)	203 (43.3%)		
WHO functional class*	1	0 (0.0%)	7 (1.7%)	1 (100.0%)	0 (0.0%)	8 (1.7%)	2.12e-10	2.23e-9	2 (1.5%)	6 (1.8%)	8 (1.7%)	0.033	0.12
	2	9 (19.1%)	74 (17.8%)	0 (0.0%)	0 (0.0%)	83 (17.5%)			14 (10.4%)	69 (20.7%)	83 (17.7%)		
	3	32 (68.1%)	263 (63.4%)	0 (0.0%)	6 (60.0%)	301 (63.6%)			96 (71.1%)	205 (61.4%)	301 (64.2%)		
	4	5 (10.6%)	51 (12.3%)	0 (0.0%)	4 (40.0%)	60 (12.7%)			22 (16.3%)	38 (11.4%)	60 (12.8%)		
Clinical indications of autoimmunity													
Comorbid hypothyroidism	No	41 (87.2%)	355 (85.5%)	1 (100.0%)	9 (90.0%)	406 (85.8%)	0.94	0.99	121 (89.6%)	281 (84.1%)	402 (85.7%)	0.16	0.36
	Yes	6 (12.8%)	60 (14.5%)	0 (0.0%)	1 (10.0%)	67 (14.2%)			14 (10.4%)	53 (15.9%)	67 (14.3%)		

Comorbid diabetes mellitus type 1	No	47 (100.0%)	408 (98.3%)	1 (100.0%)	10 (100.0%)	466 (98.5%)	0.8029	0.9876	133 (98.5%)	329 (98.5%)	462 (98.5%)	1.00	1.00
	Yes	0 (0.0%)	7 (1.7%)	0 (0.0%)	0 (0.0%)	7 (1.5%)			2 (1.5%)	5 (1.5%)	7 (1.5%)		
Comorbid Sjögren's	No	46 (97.9%)	414 (99.8%)	1 (100.0%)	10 (100.0%)	471 (99.6%)	0.31	0.92	135 (100.0%)	332 (99.4%)	467 (99.6%)	0.91	0.95
	Yes	1 (2.1%)	1 (0.2%)	0 (0.0%)	0 (0.0%)	2 (0.4%)			0 (0.0%)	2 (0.6%)	2 (0.4%)		
Comorbid ankylosing spondylitis	No	47 (100.0%)	414 (99.8%)	1 (100.0%)	10 (100.0%)	472 (99.8%)	0.99	0.99	134 (99.3%)	334 (100.0%)	468 (99.8%)	0.64	0.75
	Yes	0 (0.0%)	1 (0.2%)	0 (0.0%)	0 (0.0%)	1 (0.2%)			1 (0.7%)	0 (0.0%)	1 (0.2%)		
Comorbid polymyalgia rheumatica	No	47 (100.0%)	414 (99.8%)	1 (100.0%)	10 (100.0%)	472 (99.8%)	0.99	0.99	134 (99.3%)	334 (100.0%)	468 (99.8%)	0.64	0.75
	Yes	0 (0.0%)	1 (0.2%)	0 (0.0%)	0 (0.0%)	1 (0.2%)			1 (0.7%)	0 (0.0%)	1 (0.2%)		
Clinical autoimmunity suspicion/evidence*	No	26 (55.3%)	239 (57.6%)	1 (100.0%)	6 (60.0%)	272 (57.5%)	0.81	0.99	99 (73.3%)	173 (51.8%)	272 (58.0%)	0.42	0.64
	Yes	6 (12.8%)	43 (10.4%)	0 (0.0%)	2 (20.0%)	51 (10.8%)			15 (11.1%)	36 (10.8%)	51 (10.9%)		
Autoantibody status													
ANA*	Negative	30 (81.1%)	260 (82.8%)	1 (100.0%)	7 (87.5%)	298 (82.8%)	0.99	0.99	97 (84.3%)	201 (82.0%)	298 (82.8%)	0.83	0.91
	Positive	4 (10.8%)	31 (9.9%)	0 (0.0%)	1 (12.5%)	36 (10.0%)			11 (9.6%)	25 (10.2%)	36 (10.0%)		
Anti-cardiolipin*	Negative	16 (45.7%)	141 (45.8%)	1 (100.0%)	2 (28.6%)	160 (45.6%)	0.83	0.99	60 (52.6%)	100 (42.2%)	160 (45.6%)	0.17	0.36
	Positive	0 (0.0%)	5 (1.6%)	0 (0.0%)	0 (0.0%)	5 (1.4%)			1 (0.9%)	4 (1.7%)	5 (1.4%)		
Anti-dsDNA*	Negative	21 (58.3%)	148 (50.0%)	0 (0.0%)	2 (25.0%)	171 (50.1%)	0.61	0.99	51 (47.2%)	120 (51.5%)	171 (50.1%)	0.35	0.58
	Positive	0 (0.0%)	3 (1.0%)	0 (0.0%)	0 (0.0%)	3 (0.9%)			2 (1.9%)	1 (0.4%)	3 (0.9%)		
Anti-SCL-70*	Negative	12 (32.4%)	129 (41.0%)	1 (100.0%)	3 (37.5%)	145 (40.2%)	0.85	0.99	51 (44.0%)	94 (38.4%)	145 (40.2%)	0.49	0.68
	Positive	0 (0.0%)	1 (0.3%)	0 (0.0%)	0 (0.0%)	1 (0.3%)			0 (0.0%)	1 (0.4%)	1 (0.3%)		
Anti-centromere*	Negative	15 (40.5%)	136 (43.0%)	1 (100.0%)	2 (25.0%)	154 (42.5%)	0.85	0.99	55 (47.4%)	99 (40.2%)	154 (42.5%)	0.36	0.58
	Positive	0 (0.0%)	1 (0.3%)	0 (0.0%)	0 (0.0%)	1 (0.3%)			0 (0.0%)	1 (0.4%)	1 (0.3%)		
Anti-Rho*	Negative	11 (30.6%)	117 (37.0%)	1 (100.0%)	3 (37.5%)	132 (36.6%)	0.79	0.99	49 (42.6%)	83 (33.7%)	132 (36.6%)	0.24	0.46
	Positive	0 (0.0%)	5 (1.6%)	0 (0.0%)	0 (0.0%)	5 (1.4%)			1 (0.9%)	4 (1.6%)	5 (1.4%)		
Anti-ENA*	Negative	21 (56.8%)	183 (58.1%)	1 (100.0%)	2 (25.0%)	207 (57.3%)	0.41	0.99	57 (49.1%)	150 (61.2%)	207 (57.3%)	0.094	0.25
	Positive	1 (2.7%)	2 (0.6%)	0 (0.0%)	0 (0.0%)	3 (0.8%)			1 (0.9%)	2 (0.8%)	3 (0.8%)		
ANCA*	Negative	23 (62.2%)	149 (47.6%)	0 (0.0%)	2 (28.6%)	174 (48.6%)	0.30	0.92	46 (40.7%)	128 (52.2%)	174 (48.6%)	0.087	0.25
	Positive	1 (2.7%)	10 (3.2%)	0 (0.0%)	1 (14.3%)	12 (3.4%)			3 (2.7%)	9 (3.7%)	12 (34%)		

*Missing / not available data: Case status n = 4; PAWP n= 71; PVR n = 77; mPAP n = 21; REVEAL risk n = 118; WHO classification n = 21; Clinical autoimmunity evidence / suspicion n = 150; Annti-nuclear antibody (ANA): n =150; Anti-cardiolipin n = 308; Anti-dsDNA n = 299; Anti-SCL70 n = 327; Anti-centromere n = 318; Anti-Rho n = 336; Anti-Extractable nuclear antigen (ENA) n = 263; Anti-neutrophil cytoplasmic antibodies (ANCA) n = 287

Supplementary Table E5: Differences in autoantibody positivity between cases and controls. Autoantibody positivity was defined as 0.75Q + 2IQR of the control population. Differences in positivity ratio were compared using a Chi-square test. To control for multiple hypothesis testing, FDR-adjusted q-values were calculated across 19 tests using the Benjamini and Hochberg procedure, and resultant q values are presented. We report here as significant tests $q < 0.05$. Data shown as counts (percentage per group).

Autoantibody	Autoantibody Positivity	Healthy controls (n=946)	PAH patients (n=473)	Total (n=1419)	FDR-adjusted q-value
Cardiolipin	Negative	853 (90.2%)	366 (77.4%)	1219 (85.9%)	< 1e-04
	Positive	93 (9.8%)	107 (22.6%)	200 (14.1%)	
Centromere protein B	Negative	877 (92.7%)	444 (93.9%)	1321 (93.1%)	0.65
	Positive	69 (7.3%)	29 (6.1%)	98 (6.9%)	
H2a (F2a2) & H4 (F2a1)	Negative	870 (92.0%)	408 (86.3%)	1278 (90.1%)	0.0027
	Positive	76 (8.0%)	65 (13.7%)	141 (9.9%)	
Histone type IIa	Negative	868 (91.8%)	439 (92.8%)	1307 (92.1%)	0.70
	Positive	78 (8.2%)	34 (7.2%)	112 (7.9%)	
Jo-1	Negative	913 (96.5%)	448 (94.7%)	1361 (95.9%)	0.22
	Positive	33 (3.5%)	25 (5.3%)	58 (4.1%)	
Mi-2b	Negative	885 (93.6%)	433 (91.5%)	1318 (92.9%)	0.29
	Positive	61 (6.4%)	40 (8.5%)	101 (7.1%)	
La/SS-B	Negative	836 (88.4%)	352 (74.4%)	1188 (83.7%)	< 1e-04
	Positive	110 (11.6%)	121 (25.6%)	231 (16.3%)	
Myeloperoxidase	Negative	874 (92.4%)	433 (91.5%)	1307 (92.1%)	0.74
	Positive	72 (7.6%)	40 (8.5%)	112 (7.9%)	
Proteinase-3	Negative	894 (94.5%)	373 (78.9%)	1267 (89.3%)	< 1e-04
	Positive	52 (5.5%)	100 (21.1%)	152 (10.7%)	
Pyruvate dehydrogenase	Negative	869 (91.9%)	418 (88.4%)	1287 (90.7%)	0.072
	Positive	77 (8.1%)	55 (11.6%)	132 (9.3%)	
RNP-complex	Negative	855 (90.4%)	372 (78.6%)	1227 (86.5%)	< 1e-04
	Positive	91 (9.6%)	101 (21.4%)	192 (13.5%)	
Ro/SS-A antigen	Negative	864 (91.3%)	454 (96.0%)	1318 (92.9%)	0.0040
	Positive	82 (8.7%)	19 (4.0%)	101 (7.1%)	
SCL-70 antigen	Negative	856 (90.5%)	424 (89.6%)	1280 (90.2%)	0.74
	Positive	90 (9.5%)	49 (10.4%)	139 (9.8%)	
Scl-34	Negative	841 (88.9%)	417 (88.2%)	1258 (88.7%)	0.74
	Positive	105 (11.1%)	56 (11.8%)	161 (11.3%)	
Smith antigen	Negative	863 (91.2%)	386 (81.6%)	1249 (88.0%)	< 1e-04
	Positive	83 (8.8%)	87 (18.4%)	170 (12.0%)	
Thyroglobulin	Negative	891 (94.2%)	422 (89.2%)	1313 (92.5%)	0.0028
	Positive	55 (5.8%)	51 (10.8%)	106 (7.5%)	

Thyroid peroxidase	Negative	762 (80.5%)	349 (73.8%)	1111 (78.3%)	0.0084
	Positive	184 (19.5%)	124 (26.2%)	308 (21.7%)	
Transglutaminase	Negative	896 (94.7%)	445 (94.1%)	1341 (94.5%)	0.74
	Positive	50 (5.3%)	28 (5.9%)	78 (5.5%)	
u1-snRNP 68	Negative	893 (94.4%)	408 (86.3%)	1301 (91.7%)	< 1e-04
	Positive	53 (5.6%)	65 (13.7%)	118 (8.3%)	

Supplementary Table E6: Differences in autoantibody positivity in PAH patients between clusters. Stratification of autoantibody positivity between clustered groups. PAM with K=3 was defined as optimal after clustering and differences in prevalence of statistical autoantibody positivity were assessed with a Chi-square test. To control for multiple hypothesis testing, FDR q-values were calculated across 19 tests using the Benjamini and Hochberg procedure, Resultant q values are presented. We report here as significant tests $q < 0.05$.

Autoantibody	Positivity	High autoantibody cluster (n=130)	Low autoantibody cluster (n=290)	Intermediate autoantibody cluster (n=53)	Total (n=473)	FDR-adjusted q-value
Cardiolipin	Negative	46 (35.4%)	279 (96.2%)	41 (77.4%)	366 (77.4%)	0.00079
	Positive	84 (64.6%)	11 (3.8%)	12 (22.6%)	107 (22.6%)	
CENP-B	Negative	116 (89.2%)	280 (96.6%)	48 (90.6%)	444 (93.9%)	0.011
	Positive	14 (10.8%)	10 (3.4%)	5 (9.4%)	29 (6.1%)	
H2a & H4	Negative	78 (60.0%)	288 (99.3%)	42 (79.2%)	408 (86.3%)	0.00079
	Positive	52 (40.0%)	2 (0.7%)	11 (20.8%)	65 (13.7%)	
Histone-IIa	Negative	106 (81.5%)	287 (99.0%)	46 (86.8%)	439 (92.8%)	0.00079
	Positive	24 (18.5%)	3 (1.0%)	7 (13.2%)	34 (7.2%)	
Jo-1	Negative	115 (88.5%)	285 (98.3%)	48 (90.6%)	448 (94.7%)	0.00079
	Positive	15 (11.5%)	5 (1.7%)	5 (9.4%)	25 (5.3%)	
Mi-2b	Negative	114 (87.7%)	271 (93.4%)	48 (90.6%)	433 (91.5%)	0.15
	Positive	16 (12.3%)	19 (6.6%)	5 (9.4%)	40 (8.5%)	
La/SS-B	Negative	42 (32.3%)	268 (92.4%)	42 (79.2%)	352 (74.4%)	0.00079
	Positive	88 (67.7%)	22 (7.6%)	11 (20.8%)	121 (25.6%)	
Myeloperoxidase	Negative	109 (83.8%)	277 (95.5%)	47 (88.7%)	433 (91.5%)	0.0015
	Positive	21 (16.2%)	13 (4.5%)	6 (11.3%)	40 (8.5%)	
Proteinase-3	Negative	45 (34.6%)	285 (98.3%)	43 (81.1%)	373 (78.9%)	0.00079
	Positive	85 (65.4%)	5 (1.7%)	10 (18.9%)	100 (21.1%)	
Pyruvate dehydrogenase	Negative	107 (82.3%)	265 (91.4%)	46 (86.8%)	418 (88.4%)	0.030
	Positive	23 (17.7%)	25 (8.6%)	7 (13.2%)	55 (11.6%)	
RNP-complex	Negative	95 (73.1%)	277 (95.5%)	0 (0.0%)	372 (78.6%)	0.00079
	Positive	35 (26.9%)	13 (4.5%)	53 (100.0%)	101 (21.4%)	
Ro/SS-A	Negative	120 (92.3%)	286 (98.6%)	48 (90.6%)	454 (96.0%)	0.0027
	Positive	10 (7.7%)	4 (1.4%)	5 (9.4%)	19 (4.0%)	
SCL-70	Negative	113 (86.9%)	262 (90.3%)	49 (92.5%)	424 (89.6%)	0.47
	Positive	17 (13.1%)	28 (9.7%)	4 (7.5%)	49 (10.4%)	
Scl-34	Negative	117 (90.0%)	252 (86.9%)	48 (90.6%)	417 (88.2%)	0.59
	Positive	13 (10.0%)	38 (13.1%)	5 (9.4%)	56 (11.8%)	

Smith antigen	Negative	81 (62.3%)	267 (92.1%)	38 (71.7%)	386 (81.6%)	0.00079
	Positive	49 (37.7%)	23 (7.9%)	15 (28.3%)	87 (18.4%)	
Thyroglobulin	Negative	85 (65.4%)	290 (100.0%)	47 (88.7%)	422 (89.2%)	0.00079
	Positive	45 (34.6%)	0 (0.0%)	6 (11.3%)	51 (10.8%)	
Thyroid peroxidase	Negative	33 (25.4%)	276 (95.2%)	40 (75.5%)	349 (73.8%)	0.00079
	Positive	97 (74.6%)	14 (4.8%)	13 (24.5%)	124 (26.2%)	
Transglutaminase	Negative	110 (84.6%)	284 (97.9%)	51 (96.2%)	445 (94.1%)	0.00079
	Positive	20 (15.4%)	6 (2.1%)	2 (3.8%)	28 (5.9%)	
u1-snRNP	Negative	79 (60.8%)	285 (98.3%)	44 (83.0%)	408 (86.3%)	0.00079
	Positive	51 (39.2%)	5 (1.7%)	9 (17.0%)	65 (13.7%)	

Supplementary Table E7. Demographic and clinical characteristics of autoantibody cluster analysis in PAH patients. Numeric data shown as mean \pm standard deviation unless otherwise stated. Count data is represented as the count (percentage of total). Statistical analysis was performed using Chi-square tests and ANOVAs. To control for multiple hypothesis testing, FDR adjusted q-values were calculated across 178 tests using the Benjamini and Hochberg procedure, and resultant q values are presented. We report here as significant tests $q < 0.05$. Significant FDR corrected numeric tests were subsequently subjected by ANCOVA analysis and corrected for sex, aetiology, age at diagnosis and BMI followed by Bonferroni correction for three tests. Log_e TSH levels were used for statistical analysis however numeric values are stated for observed levels. A mutation was defined as a minor allele frequency $< 1:10,000$ in one of the following genes: *KDR*, *BMPR2*, *EIF2AK4*, *SMAD4*, *ACVRL1*, *AQP1*, *ATP13A3*, *SMAD1*, *SMAD9*, *ENG*, *GDF2*, *KCNK3*, *SOX17*, and *TBX4*.

	High autoantibody cluster (n=130)	Low autoantibody cluster (n=290)	Intermediate autoantibody cluster (n=53)	Total (n=473)	p-value	FDR-adjusted q-value	Bonferroni (For ANCOVA)
Age at diagnosis*	44.3 \pm 15.3	48.9 \pm 17.1	49 \pm 15.9	47.6 \pm 16.6	0.028	0.13	
Age at sampling	50.8 \pm 14.5	53.8 \pm 16.2	54.8 \pm 14.8	53 \pm 15.6	0.14	0.32	
Sex							
Male	31 (23.8%)	95 (32.8%)	15 (28.3%)	141 (29.8%)	0.18	0.37	
Female	99 (76.2%)	195 (67.2%)	38 (71.7%)	332 (70.2%)			
BMI \pm kg/m ² *	27.8 \pm 6.3	28.9 \pm 7.1	30.7 \pm 7.6	28.8 \pm 7	0.043	0.17	
Diagnosis							
HPAH	10 (7.7%)	32 (11.0%)	5 (9.4%)	47 (9.9%)	0.70	0.83	
IPAH	118 (90.8%)	249 (85.9%)	48 (90.6%)	415 (87.7%)			
PVOD	0 (0.0%)	1 (0.3%)	0 (0.0%)	1 (0.2%)			
PCH	2 (1.5%)	8 (2.8%)	0 (0.0%)	10 (2.1%)			
Mutations*							
Total PAH relevant mutation frequency	24 (18.5%)	82 (28.3%)	9 (17.0%)	115 (24.3%)	0.014	0.087	
BMPR2 mutation frequency	18 (13.8%)	53 (18.3%)	5 (9.4%)	76 (16.1%)	0.11	0.28	
Haemodynamics							
mPAP \pm mmHg*	54.5 (12.9)	52.9 (13.4)	51.9 (12.1)	53.2 (13.1)	0.39	0.59	
mPAWP \pm mmHg*	8.5 (4)	9.7 (3.6)	9.4 (4.1)	9.3 (3.8)	0.028	0.13	

mRAP ± mmHg*	9 (5.6)	9.1 (5.1)	8.5 (5.3)	9 (5.2)	0.73	0.83	
Cardiac output ± l/min *	3.7 (1.3)	4.1 (1.3)	4.4 (1.5)	4 (1.4)	0.0024	0.018	0.0084
Cardiac index*	2.1 (0.7)	2.2 (0.7)	2.4 (0.8)	2.2 (0.7)	0.022	0.12	
TSH ± mu/l*	3.5 (3.7)	2.1 (1.5)	2.8 (2.9)	2.6 (2.5)	0.066	0.20	
PVR ± Wood units*	14 (6.5)	11.7 (5.4)	10.8 (5.1)	12.2 (5.8)	0.00075	0.0063	0.0051
PVR-calc ± dynes-sec/cm ⁵ *	1119.4 (528)	941.4 (437.7)	858.2 (445)	980.9 (471.9)	0.00067	0.0060	0.022
6MWD distance ± meters*	341.4 (161)	314.8 (155.6)	306.4 (154.4)	321.1 (157.1)	0.25	0.51	
spO ₂ pre-6MWD *	95.7 (3.1)	94.5 (4.1)	94.6 (4.1)	94.9 (3.9)	0.026	0.12	
spO ₂ post-6MWD	91.9 (7.3)	89.4 (8.4)	88.1 (9.3)	90 (8.3)	0.013	0.083	
WHO functional class*					0.0059	0.042	
1	4 (3.1%)	3 (1.0%)	1 (1.9%)	8 (1.7%)			
2	23 (17.7%)	48 (16.6%)	12 (22.6%)	83 (17.5%)			
3	67 (51.5%)	196 (67.6%)	38 (71.7%)	301 (63.6%)			
4	26 (20.0%)	33 (11.3%)	1 (1.9%)	60 (12.7%)			
REVEAL Risk Score*					0.092	0.25	
Low	55 (42.3%)	119 (41.0%)	29 (54.7%)	203 (42.9%)			
Moderate	10 (7.7%)	51 (17.6%)	6 (11.3%)	67 (14.2%)			
High	20 (15.4%)	42 (14.5%)	3 (5.7%)	65 (13.7%)			
Very high	5 (3.8%)	13 (4.5%)	2 (3.8%)	20 (4.2%)			
Indications of autoimmune disease							
Co-morbid hypothyroidism					4.5e-6	4.2e-5	
Yes	33 (25.4%)	23 (7.9%)	11 (20.8%)	67 (14.2%)			
No	97 (74.6%)	267 (92.1%)	42 (79.2%)	406 (85.8%)			
Diabetes Mellitus type 1					0.63	0.77	
Yes	2 (1.5%)	5 (1.7%)	0 (0.0%)	7 (1.5%)			
No	128 (98.5%)	285 (98.3%)	53 (100.0%)	466 (98.5%)			
Sjögren's					0.071	0.20	
Yes	2 (1.5%)	0 (0.0%)	0 (0.0%)	2 (0.4%)			
No	128 (98.5%)	290 (100.0%)	53 (100.0%)	471 (99.6%)			
Ankylosing Spondylitis					0.73	0.83	
Yes	0 (0.0%)	1 (0.3%)	0 (0.0%)	1 (0.2%)			
No	130 (100.0%)	289 (99.7%)	53 (100.0%)	472 (99.8%)			
Polymyalgia rheumatica					0.73	0.83	
Yes	0 (0.0%)	1 (0.3%)	0 (0.0%)	1 (0.2%)			
No	130 (100.0%)	289 (99.7%)	53 (100.0%)	472 (99.8%)			
Overlap syndrome					0.73	0.83	
Yes	0 (0.0%)	1 (0.3%)	0 (0.0%)	1 (0.2%)			
No	130 (100.0%)	289 (99.7%)	53 (100.0%)	472 (99.8%)			

Clinical autoimmunity suspicion / evidence*					0.12	0.28	
Yes	16 (12.3%)	26 (9.0%)	9 (17.0%)	51 (10.8%)			
No	71 (54.6%)	175 (60.3%)	26 (49.1%)	272 (57.5%)			
Autoantibodies							
ANA*					0.16	0.36	
Positive	12 (9.2%)	17 (5.9%)	7 (13.2%)	36 (7.6%)			
Negative	79 (60.7%)	186 (64.1%)	33 (62.3%)	298 (63.0%)			
ANCA*					0.83	0.89	
Positive	3 (2.3%)	8 (2.8%)	1 (1.9%)	12 (2.5%)			
Negative	47 (36.2%)	103 (35.5%)	24 (45.3%)	174 (36.8%)			
Anti-Cardiolipin*					0.24	0.49	
Positive	3 (2.3%)	2 (0.7%)	0 (0.0%)	5 (1.1%)			
Negative	43 (33.1%)	98 (33.8%)	19 (35.8%)	160 (33.8%)			
Anti-dsDNA*					0.018	0.10	
Positive	3 (2.3%)	0 (0.0%)	0 (0.0%)	3 (0.6%)			
Negative	45 (34.6%)	105 (36.2%)	21 (39.6%)	171 (36.2%)			
Anti-SCL70*					0.38	0.59	
Positive	1 (0.8%)	0 (0.0%)	0 (0.0%)	1 (0.2%)			
Negative	49 (37.7%)	82 (28.3%)	14 (26.4%)	145 (30.7%)			
Anti-centromere*					0.013	0.083	
Positive	0 (0.0%)	0 (0.0%)	1 (1.9%)	1 (0.2%)			
Negative	44 (33.8%)	95 (32.8%)	15 (28.3%)	154 (32.6%)			
Anti-Rho*					0.088	0.24	
Positive	4 (3.1%)	1 (0.3%)	0 (0.0%)	5 (1.1%)			
Negative	43 (33.1%)	77 (26.6%)	12 (22.6%)	132 (27.9%)			
Anti-ENA*					0.28	0.52	
Positive	2 (1.5%)	1 (0.3%)	0 (0.0%)	3 (0.6%)			
Negative	54 (41.5%)	128 (44.1%)	25 (47.2%)	207 (43.8%)			
Other relevant comorbidities							
Type 2 diabetes mellitus					0.0039	0.029	
Yes	7 (5.4%)	46 (15.9%)	11 (20.8%)	64 (13.5%)			
No	123 (94.6%)	244 (84.1%)	42 (79.2%)	409 (86.5%)			
Treatment							
Type of treatment					0.026	0.12	
No medication recorded	5 (3.8%)	13 (4.5%)	0 (0.0%)	18 (3.8%)			
Single therapy	15 (11.5%)	33 (11.4%)	6 (11.3%)	54 (11.4%)			
Combination therapy	23 (17.7%)	82 (28.3%)	20 (37.7%)	125 (26.4%)			
Triple therapy	54 (41.5%)	123 (42.4%)	20 (37.7%)	197 (41.6%)			
Intravenous medication	33 (25.4%)	39 (13.4%)	7 (13.2%)	79 (16.7%)			

*Missing data: age at diagnosis n=4, BMI n=24, BMPR2 mutation frequency = 74, mPAP n=21, mPAWP n=73, mRAP n=41, cardiac output n=37, cardiac index n=47, TSH n=138, PVR n=77, PVR-calc n=61, 6MWD n=50, spO₂ pre 6MWD n=65, WHO functional class n=21, REVEAL risk score n= 118, Clinical autoimmunity suspicion / evidence n=150, ANA n=139, ANCA n=287, anti-cardiolipin n=308, anti-dsDNA n=299, anti-SCL70 n=327, anti-centromere n=318, anti-Rho n=336, anti-ENA n=263

BMI (Body Mass Index); mPAP (mean Pulmonary Arterial Pressure); mRAP (mean Right Atrial Pressure); TSH (Thyroid Stimulating Hormone); PVR (Pulmonary Vascular Resistance); PVR-calc (calculated PVR); 6MWD (six minutes walking distance test); spO₂ (oxygen saturation); ANA (anti-nuclear antibodies); ANCA (anti-neutrophil cytoplasmic antibodies); anti-ENA (anti – extractable nuclear antigen).

Supplementary Results Figures - Legends

Supplementary Figure E4: Correlation analysis of lymphocytes; CD3⁺; CD4⁺ T cell and CD8⁺ T cell populations measured across different immunophenotyping panels. Samples from individuals were measured across multiple antibody panels and show good correlation. P values and r or r² were derived by Pearson or Spearman's rank correlation determined by normality of data.

Supplementary Figure E5: Correlations of leukocyte cell populations in IPAH patients. A) T_{REG} vs. Plasmablast; B) T_{REG} vs. circulating T_{FH}; C) Non-switched memory B cells vs. Plasmablasts. P values and r calculations derived from Pearson or Spearman's rank correlation depending on normality of data.

Supplementary Figure E6: Cox-proportional hazard model of survival differences between clusters. Survival differences between clusters were corrected for age at diagnosis, sex and treatment using a cox-proportional hazard model. Wald tests were used to determine p-values.

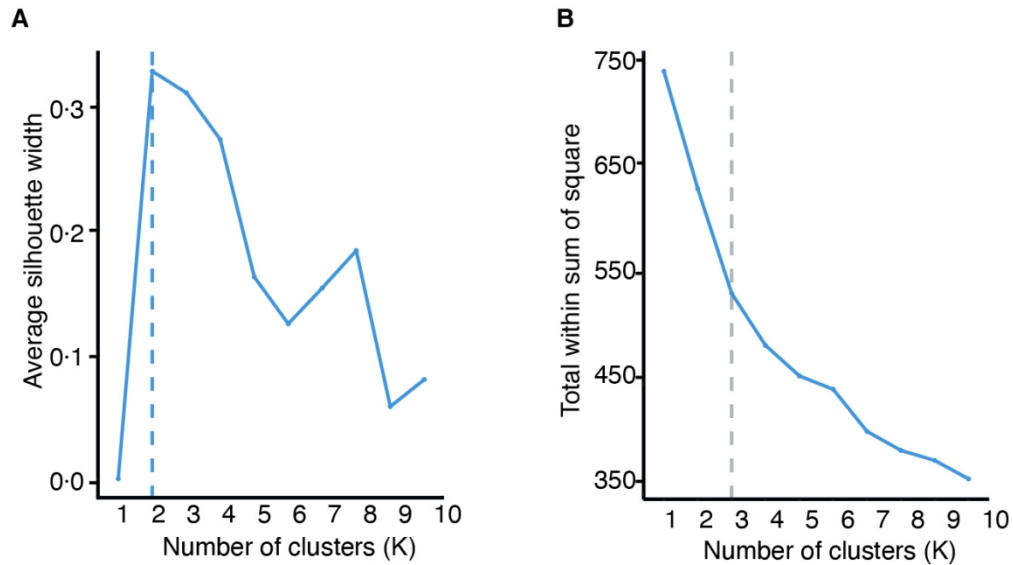


Figure E2: Assessment of optimal number of clusters for autoantibody clustering.

A) Silhouette plot; B) Elbow plot of Loge transformed autoantibody levels for PAM clustering with Euclidean distances. The silhouette plot and elbow plot indicate the optimal number of clusters (K) for PAM clustering with Euclidean distances. In A) the best performance is seen for $K = 2$, with $K = 3$ being a close second. In

B) the first bend in the plot is seen at $K = 3$ with another at $K = 5$. The combination of these results suggests that $K = 3$ is the optimal choice for clustering, which fits with clinical expectations.

111x62mm (300 x 300 DPI)

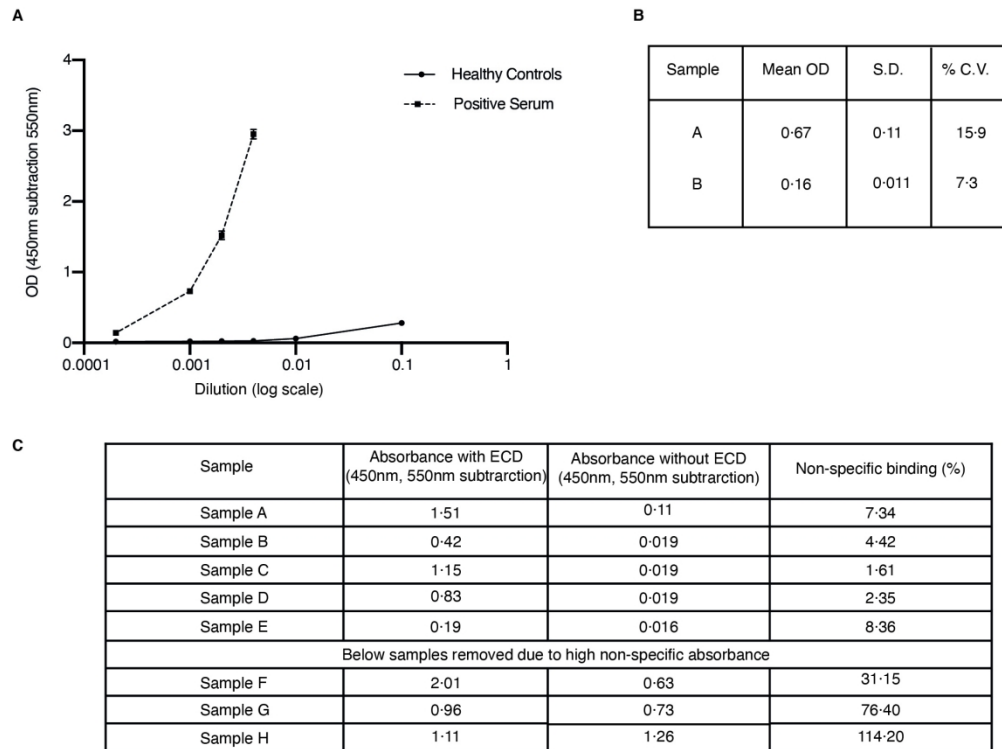
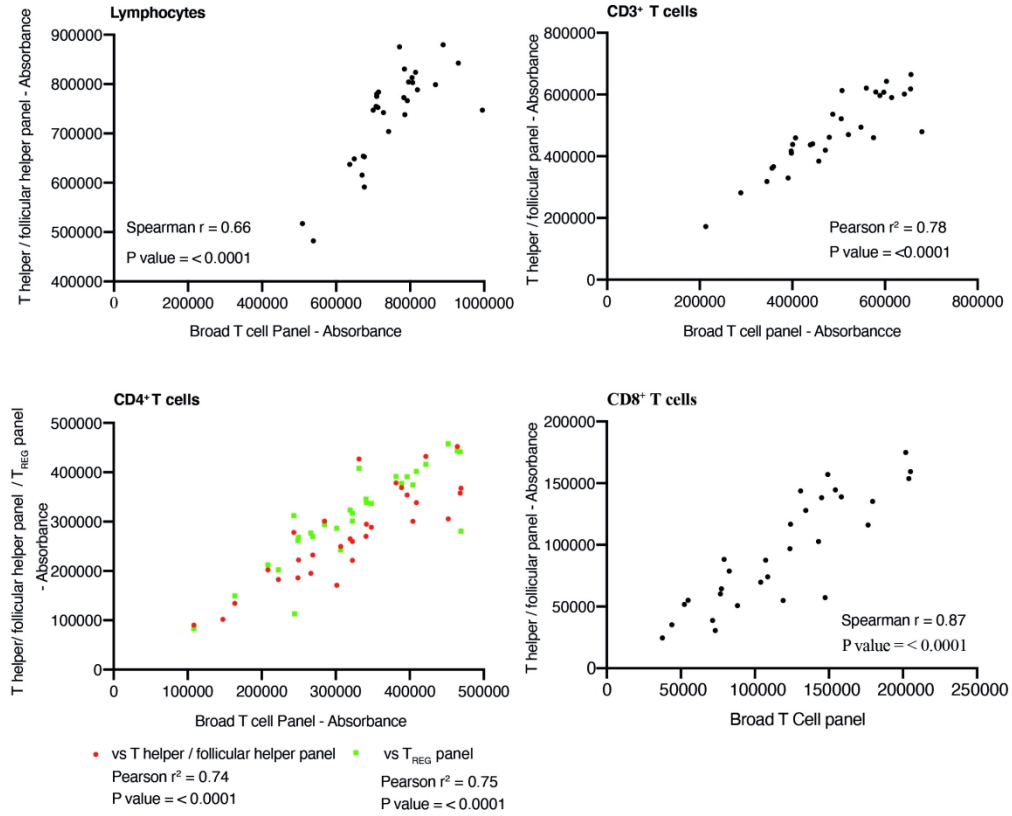


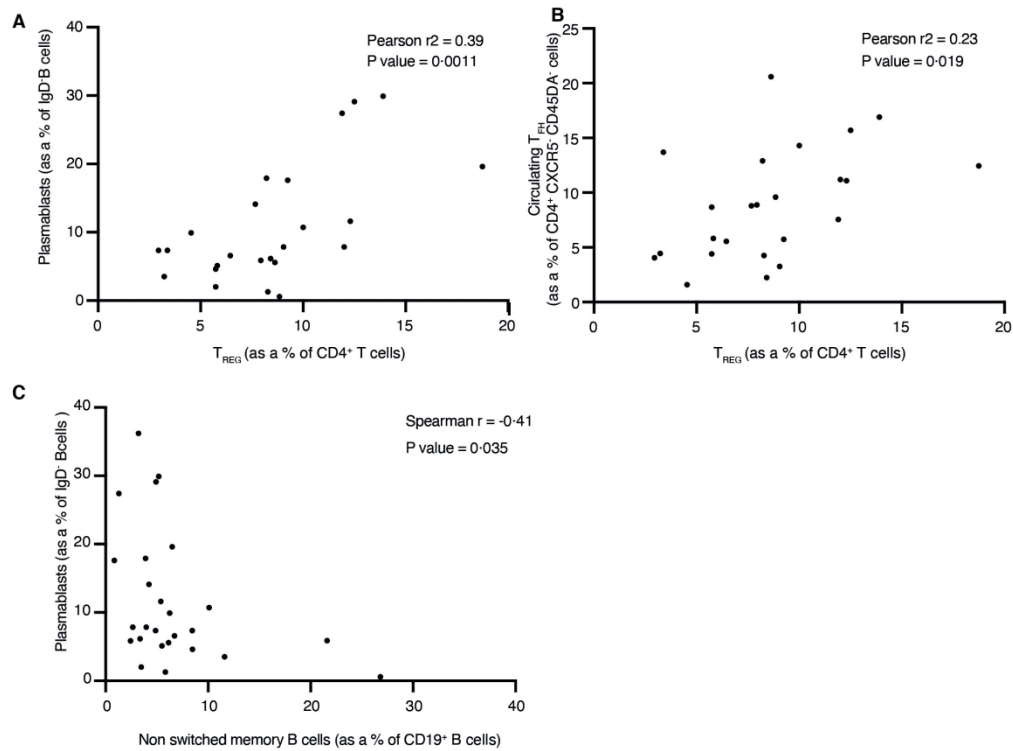
Figure E3: Development of a novel ELISA for the detection of autoantibodies to the Bmpr2 extracellular domain (ECD). A) Serum from a healthy donor and a PAH patient demonstrating IgG reactivity was titrated to determine optimal sample dilution. B) Co-efficient of variation of two PAH samples shows good inter-plate variation, co-efficient of variation shown as % CV. C) Examples of test for non-specific binding of patient serum demonstrating IgG reactivity to the Bmpr2 ECD. Samples were incubated both in the presence and absence of ECD and calculated as percentage binding. Sera with high levels of non-specific absorbance were removed.

179x133mm (300 x 300 DPI)



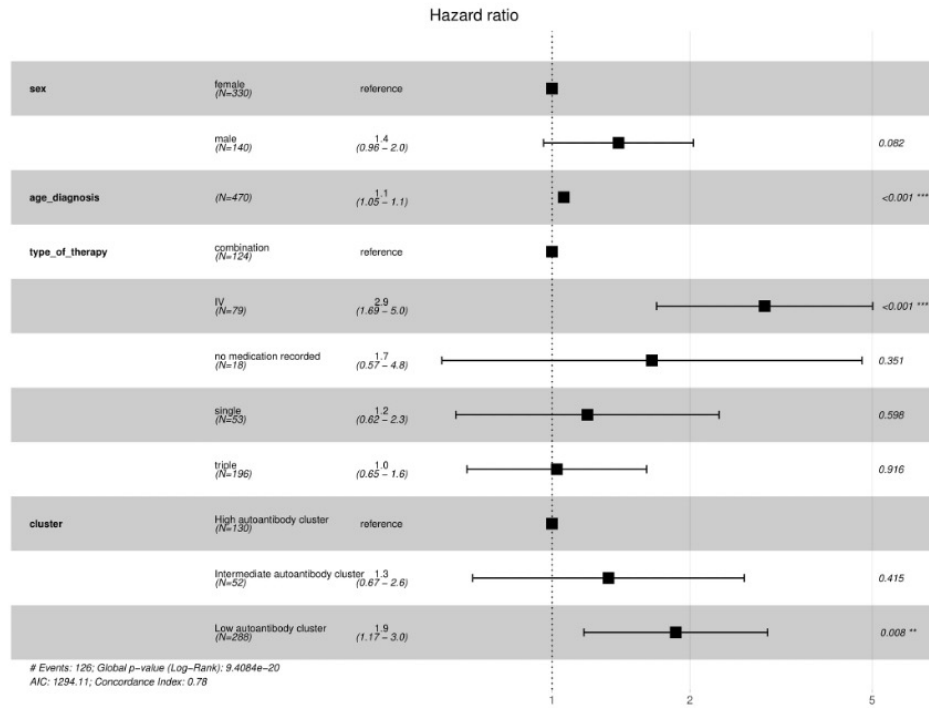
Supplementary Figure E4: Correlation analysis of lymphocytes; CD3+; CD4+ T cell and CD8+ T cell populations measured across different immunophenotyping panels. Samples from individuals were measured across multiple antibody panels and show good correlation. P values and r or r2 were derived by Pearson or Spearman’s rank correlation determined by normality of data.

205x168mm (300 x 300 DPI)



Supplementary Figure E5: Correlations of leukocyte cell populations in IPAH patients. A) TREG vs. Plasmablast; B) TREG vs. circulating TFH; C) Non-switched memory B cells vs. Plasmablasts. P values and r calculations derived from Pearson or Spearman's rank correlation depending on normality of data.

185x138mm (300 x 300 DPI)



Supplementary Figure E6: Cox-proportional hazard model of survival differences between clusters. Survival differences between clusters were corrected for age at diagnosis, sex and treatment using a cox-proportional hazard model. Wald tests were used to determine p-values.

159x115mm (144 x 144 DPI)